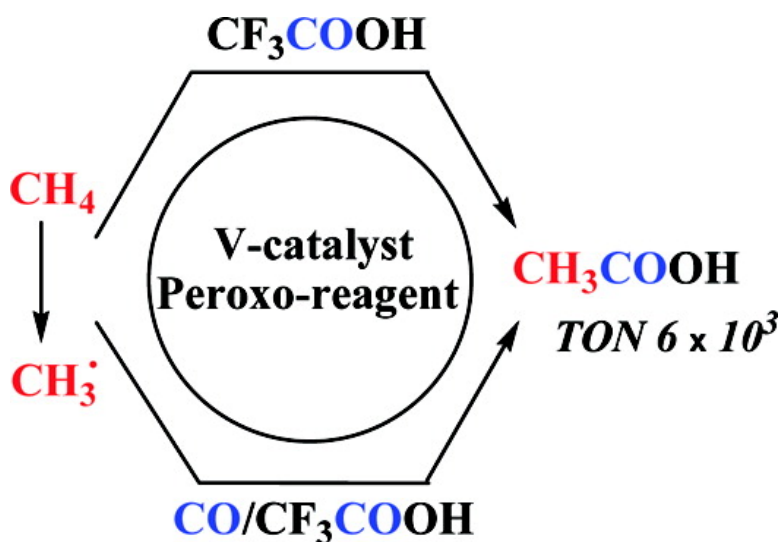


Direct and Remarkably Efficient Conversion of Methane into Acetic Acid Catalyzed by Amavadine and Related Vanadium Complexes. A Synthetic and a Theoretical DFT Mechanistic Study

Marina V. Kirillova, Maxim L. Kuznetsov, Patricia M. Reis, Jos A. L. da Silva, Joo J. R. Frasto da Silva, and Armando J. L. Pombeiro

J. Am. Chem. Soc., **2007**, 129 (34), 10531-10545 • DOI: 10.1021/ja072531u • Publication Date (Web): 04 August 2007

Downloaded from <http://pubs.acs.org> on February 15, 2009



More About This Article

Additional resources and features associated with this article are available within the HTML version:

- Supporting Information
- Links to the 3 articles that cite this article, as of the time of this article download
- Access to high resolution figures
- Links to articles and content related to this article
- Copyright permission to reproduce figures and/or text from this article

[View the Full Text HTML](#)



Direct and Remarkably Efficient Conversion of Methane into Acetic Acid Catalyzed by Amavadinone and Related Vanadium Complexes. A Synthetic and a Theoretical DFT Mechanistic Study

Marina V. Kirillova, Maxim L. Kuznetsov, Patrícia M. Reis, José A. L. da Silva, João J. R. Fraústo da Silva, and Armando J. L. Pombeiro*

Contribution from the Centro de Química Estrutural, Complexo I, Instituto Superior Técnico, TU Lisbon, Av. Rovisco Pais, 1049-001 Lisbon, Portugal

Received April 23, 2007; E-mail: pombeiro@ist.utl.pt

Abstract: Vanadium(IV or V) complexes with N,O- or O,O-ligands, i.e., $[\text{VO}\{\text{N}(\text{CH}_2\text{CH}_2\text{O})_3\}]$, $\text{Ca}[\text{V}(\text{HIDPA})_2]$ (synthetic *amavadinone*), $\text{Ca}[\text{V}(\text{HIDA})_2]$, or $[\text{Bu}_4\text{N}]_2[\text{V}(\text{HIDA})_2]$ [HIDPA, HIDA = basic form of 2,2'-(hydroxyimino)dipropionic or -diacetic acid, respectively], $[\text{VO}(\text{CF}_3\text{SO}_3)_2]$, $\text{Ba}[\text{VO}(\text{nta})(\text{H}_2\text{O})_2]$ (nta = nitrilotriacetate), $[\text{VO}(\text{ada})(\text{H}_2\text{O})]$ (ada = *N*-2-acetamidoiminodiacetate), $[\text{VO}(\text{Hheida})(\text{H}_2\text{O})]$ (Hheida = 2-hydroxyethyliminodiacetate), $[\text{VO}(\text{bicine})]$ [bicine = basic form of *N,N*-bis(2-hydroxyethyl)glycine], and $[\text{VO}(\text{dipic})(\text{OCH}_2\text{CH}_3)]$ (dipic = pyridine-2,6-dicarboxylate), are catalyst precursors for the efficient single-pot conversion of methane into acetic acid, in trifluoroacetic acid (TFA) under moderate conditions, using peroxodisulfate as oxidant. Effects on the yields and TONs of various factors are reported. TFA acts as a carbonylating agent and CO is an inhibitor for some systems, although for others there is an optimum CO pressure. The most effective catalysts (as *amavadinone*) bear triethanolamine or (hydroxyimino)dicarboxylates and lead, in a single batch, to CH_3COOH yields > 50% (based on CH_4) or remarkably high TONs up to 5.6×10^3 . The catalyst can remain active upon multiple recycling of its solution. Carboxylation proceeds via free radical mechanisms (CH_3^\bullet can be trapped by CBrCl_3), and theoretical calculations disclose a particularly favorable process involving the sequential formation of CH_3^\bullet , $\text{CH}_3\text{CO}^\bullet$, and $\text{CH}_3\text{COO}^\bullet$ which, upon H-abstraction (from TFA or CH_4), yields acetic acid. The $\text{CH}_3\text{COO}^\bullet$ radical is formed by oxygenation of $\text{CH}_3\text{CO}^\bullet$ by a peroxo-V complex via a $\text{V}\{\eta^1\text{-OOC}(\text{O})\text{CH}_3\}$ intermediate. Less favorable processes involve the oxidation of $\text{CH}_3\text{CO}^\bullet$ by the protonated (hydroperoxo) form of that peroxo-V complex or by peroxodisulfate. The calculations also indicate that (i) peroxodisulfate behaves as a source of sulfate radicals which are methane H-abstractors, as a peroxidative and oxidizing agent for vanadium, and as an oxidizing and coupling agent for $\text{CH}_3\text{CO}^\bullet$ and that (ii) TFA is involved in the formation of CH_3COOH (by carbonylating CH_3^\bullet , acting as an H-source to $\text{CH}_3\text{COO}^\bullet$, and enhancing on protonation the oxidizing power of a peroxo-V^V complex) and of $\text{CF}_3\text{-COOCH}_3$ (minor product in the absence of CO).

1. Introduction

Functionalization of C–H bonds of alkanes (in particular the gaseous ones, “noble gases of organic chemistry”¹ due to their low reactivity) has attracted much current attention, namely in connection with the search for new raw materials for the chemical industry. In particular, there has been a strong economic motivation to transform saturated hydrocarbons directly into more valuable functionalized products such as alcohols, esters, aldehydes, ketones, acids, amines, and others.^{1–13} Among these processes, the selective conversion of methane (the most abundant and unreactive hydrocarbon, the main

component of natural gas and a cheap potential raw material) to various oxidized products, such as methanol and acetic acid, is a challenging topic in both organic and bioinorganic chemistries, with a special interest in catalysis. Moreover, the development of such processes could eventually contribute to the understanding of aspects of the prebiotic chemistry in Earth (when methane was one of the major constituents of the atmosphere) and also to devising a method for lowering its concentration in the present atmosphere, which has been

- (1) Shul'pin, G. B. *J. Mol. Catal. A: Chem.* **2002**, *189*, 39.
- (2) *Activation and Functionalization of Alkanes*; Hill, C. L., Ed.; Wiley: New York, 1989.
- (3) *Methane Conversion by Oxidative Processes: Fundamental and Engineering Aspects*; Wolf, E. E., Eds.; Van Nostrand Reinhold: New York, 1992.
- (4) Periana, R. A.; Taube, D. J.; Gamble, S.; Taube, H.; Satoh, T.; Fujii, H. *Science* **1998**, *280*, 560.
- (5) Crabtree, R. H. *Chem. Rev.* **1995**, *95*, 987; Crabtree, R. H. *Chem. Rev.* **1995**, *95*, 2599.

- (6) *Catalytic Activation and Functionalization of Light Alkanes*; Derouane, E. G.; Haber, J.; Lemos, F.; Ramôa Ribeiro, F.; Guinet M., Eds.; NATO ASI series, High Technology Sub-series, Vol. 44; Kluwer Academic Publishers: Dordrecht, The Netherlands, 1998.
- (7) Mukhopadhyay, S.; Bell, A. T. *Angew. Chem., Int. Ed.* **2003**, *42*, 1019.
- (8) Mukhopadhyay, S.; Bell, A. T. *J. Am. Chem. Soc.* **2003**, *125*, 4406.
- (9) Jia, C.; Kitamura, T.; Fujiwara, Y. *Acc. Chem. Res.* **2001**, *34*, 633.
- (10) Shilov, A. E.; Shul'pin, G. B. *Chem. Rev.* **1997**, *97*, 2879.
- (11) Crabtree, R. H. *J. Chem. Soc., Dalton Trans.* **2001**, 2437.
- (12) Crabtree, R. H. *The Organometallic Chemistry of the Transition Metals*; Wiley: New York, 2001; Chapter 12.
- (13) Fujiwara, Y.; Takaki, K.; Taniguchi, Y. *Synlett* **1995**, 591.

progressively increasing as a consequence of human activity (such as sewage and rice paddies) with a resulting enhancement of the greenhouse effect.¹⁴

The production of carboxylic acids by carbonylation of organic compounds is one of the most important industrial processes in homogeneous catalysis. It involves a transition metal assisted addition of carbon monoxide to an organic substrate to yield higher molecular weight carbonyl-containing products.^{15,16} In particular, the carbonylation of methanol to produce acetic acid is quite an industrially significant process.^{15,16} The requirement of three separate stages (metal-catalyzed high-temperature steam-reforming of CH₄, conversion of the derived synthesis gas to CH₃OH, and carbonylation of CH₃OH with CO) and the usage of harsh reaction conditions (e.g., high temperatures and pressures) and of expensive catalyst systems containing either Rh or Ir compounds (Monsanto or Cativa process, respectively, for methanol carbonylation) encourage the search for other preparative routes for acetic acid.^{17–20} Since the discovery in 1992 by Fujiwara's group of the direct conversion of methane into acetic acid catalyzed by CuSO₄/Pd(OCOEt)₂ in trifluoroacetic acid (TFA) in the presence of K₂S₂O₈,²⁰ several other catalysts and routes of methane carbonylation to acetic acid or its derivatives have been reported.^{17,18,21–34} However, most of these processes and catalytic systems still display a limited efficiency providing low or modest yields (relative to methane) and low turnover numbers (TONs), even when operating under harsh conditions and based on an expensive metal catalyst, and their mechanisms remain unknown. A recent achievement is the interesting oxidative condensation of CH₄ to CH₃COOH (ca. 10% yield) at 180 °C in liquid sulfuric acid, catalyzed by Pd^{II}.¹⁷

Some of us have preliminarily reported³⁵ that methane can be easily converted (at 80 °C) into acetic acid, in the TFA/

K₂S₂O₈ system, by using vanadium catalysts such as synthetic *amavadine*, the natural complex [V(HIDPA)₂]^{2–} (HIDPA = basic form of 2,2'-(hydroxyimino)dipropionic acid) present in some *Amanita* fungi with a still unknown biological role. We now extend these studies to a variety of experimental conditions (including the use of radical traps and ¹³C-labeled species) and to other vanadium catalytic systems, aiming at the identification of the main factors and of the type of mechanism, a better understanding and the optimization of the process, and a contribution toward the search for an attractive method of methane carbonylation, namely by looking for a catalytic system capable of multiple recycling without loss of its activity.

Theoretical calculations are also performed to assist in the establishment of possible mechanisms for the carbonylation of methane, an approach that had not yet been previously addressed in detail for such a type of system. Although a number of mechanistic proposals have been recently considered for alkane hydroxylation,³⁶ halogenation,³⁷ and dehydrogenation³⁸ reactions, of methane oxidation in sulfuric acid³⁹ and on an Fe-exchanged zeolite,⁴⁰ of activation of C–H bonds of alkanes by platinum,⁴¹ titanium,⁴² and lanthanide⁴³ complexes, by dirhodium tetracarboxylate,⁴⁴ by unsaturated aluminum ions,⁴⁵ by Sc⁺ cation,⁴⁶ by metal oxides,⁴⁷ etc., to our knowledge, there are only a few publications where possible mechanisms of alkane carbonylation were proposed^{17,25,29,31,33,48} and only one case with detailed theoretical calculations^{34b} that has been reported and in a system different from ours.

(14) Kasting, J. F.; Siefert, J. L. *Science* **2002**, *296*, 1066.

(15) King, R. B. *Encyclopedia of Inorganic Chemistry*; John Wiley & Sons: New York, 1994; Vol. 2, p 217.

(16) (a) *Ullmann's Encyclopedia of Industrial Chemistry*, 6th ed.; Wiley-VCH: Weinheim, 2002. (b) *Encyclopedia of Chemical Technology*, 5th ed.; Kirk-Othmer, Wiley: 2004.

(17) Periana, R. A.; Mironov, O.; Taube, D.; Bhalla, G.; Jones, C. J. *Science* **2003**, *301*, 814.

(18) Shibamoto, A.; Sakaguchi, S.; Ishii, Y. *Tetrahedron Lett.* **2002**, *43*, 8859.

(19) Linke, D.; Wolf, D.; Baerns, M.; Timpe, O.; Schlögl, R.; Zey, S.; Dingerdissen, U. *J. Catal.* **2002**, *205*, 16.

(20) Nishiguchi, T.; Nakata, K.; Fujiwara, Y. *Chem. Lett.* **1992**, 1141.

(21) Kitamura, T.; Ishida, Y.; Yamagi, T.; Fujiwara, Y. *Bull. Chem. Soc. Jpn.* **2003**, *76*, 1677.

(22) Asadullah, M.; Kitamura, T.; Fujiwara, Y. *Angew. Chem., Int. Ed.* **2000**, *39*, 2475.

(23) Asadullah, M.; Taniguchi, Y.; Kitamura, T.; Fujiwara, Y. *Appl. Catal. A* **2000**, *194–195*, 443.

(24) Asadullah, M.; Kitamura, T.; Fujiwara, Y. *Chem. Lett.* **1999**, 449.

(25) Taniguchi, Y.; Hayashida, T.; Shibasaki, H.; Piao, D.; Kitamura, T.; Yamaji, T.; Fujiwara, Y. *Org. Lett.* **1999**, *1*, 557.

(26) Asadullah, M.; Kitamura, T.; Fujiwara, Y. *Appl. Organomet. Chem.* **1999**, *13*, 539.

(27) Asadullah, M.; Taniguchi, Y.; Kitamura, T.; Fujiwara, Y. *Tetrahedron Lett.* **1999**, *40*, 8867.

(28) Nizova, G. V.; Süß-Fink, G.; Stanislas, S.; Shul'pin, G. B. *Chem. Commun.* **1998**, 1885.

(29) Asadullah, M.; Taniguchi, Y.; Kitamura, T.; Fujiwara, Y. *Appl. Organomet. Chem.* **1998**, *12*, 277.

(30) Lin, M.; Sen, A. *Nature* **1994**, *368*, 613.

(31) Nakata, K.; Yamaoka, Y.; Miyata, T.; Taniguchi, Y.; Takaki, K.; Fujiwara, Y. *J. Organomet. Chem.* **1994**, *473*, 329.

(32) Piao, D. G.; Inoue, K.; Shibasaki, H.; Taniguchi, Y.; Kitamura, T.; Fujiwara, Y. *J. Organomet. Chem.* **1999**, *574*, 116.

(33) Zerella, M.; Mukhopadhyay, S.; Bell, A. T. *Org. Lett.* **2003**, *5*, 3193.

(34) (a) Zerella, M.; Mukhopadhyay, S.; Bell, A. T. *Chem. Commun.* **2004**, 1948. (b) Chempath, S.; Bell, A. T. *J. Am. Chem. Soc.* **2006**, *128*, 4650.

(35) Reis, P. M.; Silva, J. A. L.; Palavira, A. F.; Fraústo da Silva, J. J. R.; Kitamura, T.; Fujiwara, Y.; Pombeiro, A. J. L. *Angew. Chem., Int. Ed.* **2003**, *42*, 821.

(36) (a) Jones, C. J.; Taube, D.; Ziatdinov, V. R.; Periana, R. A.; Nielsen, R. J.; Oxgaard, J.; Goddard, W. A., III. *Angew. Chem., Int. Ed.* **2004**, *43*, 4626.

(b) Baik, M.-H.; Newcomb, M.; Friesner, R. A.; Lippard, S. J. *Chem. Rev.* **2003**, *103*, 2385. (c) Sharma, P. K.; de Visser, S. P.; Oglaro, F.; Shaik, S. *J. Am. Chem. Soc.* **2003**, *125*, 2291. (d) Oglaro, F.; Harris, N.; Cohen, S.; Filatov, M.; de Visser, S. P.; Shaik, S. *J. Am. Chem. Soc.* **2000**, *122*, 8977.

(e) Ensing, B.; Buda, F.; Gribnau, M. C. M.; Baerends, E. J. *J. Am. Chem. Soc.* **2004**, *126*, 4355. (f) Filatov, M.; Harris, N.; Shaik, S. *Angew. Chem., Int. Ed.* **1999**, *38*, 3510. (g) Harris, N.; Cohen, S.; Filatov, M.; Oglaro, F.; Shaik, S. *Angew. Chem., Int. Ed.* **2000**, *39*, 2003. (h) Yoshizawa, K. *Coord. Chem. Rev.* **2002**, *226*, 251. (i) Yoshizawa, K.; Yumura, T. *Chem.—Eur. J.* **2003**, *9*, 2347.

(37) Fokin, A. A.; Shubina, T. E.; Gunchenko, P. A.; Isaev, S. D.; Yurchenko, A. G.; Schreiner, P. R. *J. Am. Chem. Soc.* **2002**, *124*, 10718.

(38) (a) Gilardoni, F.; Bell, A. T.; Chakraborty, A.; Boulet, P. *J. Phys. Chem. B* **2000**, *104*, 12250. (b) Krogh-Jespersen, K.; Czerw, M.; Summa, N.; Renkema, K. B.; Achord, P. D.; Goldman, A. S. *J. Am. Chem. Soc.* **2002**, *124*, 11404. (c) Frash, M. V.; van Santen, R. A. *J. Phys. Chem. A* **2000**, *104*, 2468. (d) Haenel, M. W.; Oevers, S.; Angermund, K.; Kaska, W. C.; Fan, H.-J.; Hall, M. B. *Angew. Chem., Int. Ed.* **2001**, *40*, 3596. (e) Fan, H.-J.; Hall, M. B. *J. Mol. Catal. A: Chem.* **2002**, *189*, 111. (f) Furtado, E. A.; Milas, I.; Lins, J. O. M. A.; Nascimento, M. A. C. *Phys. Status Solidi A* **2001**, *187*, 275. (g) Zhang, G.; Li, S.; Jiang, Y. *Organometallics* **2003**, *22*, 3820.

(39) Goepfert, A.; Dinér, P.; Ahlberg, P.; Sommer, J. *Chem.—Eur. J.* **2002**, *8*, 3277.

(40) Liang, W.-Z.; Bell, A. T.; Head-Gordon, M.; Chakraborty, A. K. *J. Phys. Chem. B* **2004**, *108*, 4362.

(41) Kua, J.; Xu, X.; Periana, R. A.; Goddard, W. A., III. *Organometallics* **2002**, *21*, 511.

(42) (a) Cundari, T. R.; Klinckman, T. R.; Wolczanski, P. T. *J. Am. Chem. Soc.* **2002**, *124*, 1481. (b) Ustynyuk, L. Yu.; Ustynyuk, Yu. A.; Laikov, D. N.; Lunin, V. V. *Russ. Chem. Bull.* **2001**, *50*, 376.

(43) Maron, L.; Perrin, L.; Eisenstein, O. *J. Chem. Soc., Dalton Trans.* **2002**, 534.

(44) Nakamura, E.; Yoshikai, N.; Yamanaka, M. *J. Am. Chem. Soc.* **2002**, *124*, 7181.

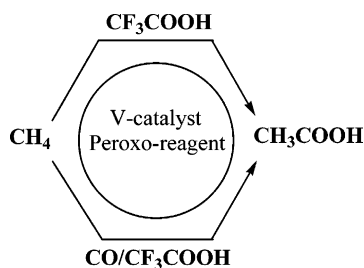
(45) Fărcașiu, D.; Lukinskas, P. *J. Phys. Chem. A* **2002**, *106*, 1619.

(46) Zhang, D.; Liu, C.; Bi, S.; Yuan, S. *Chem.—Eur. J.* **2003**, *9*, 484.

(47) (a) Hwang, D. Y.; Mebel, A. M. *J. Phys. Chem. A* **2002**, *106*, 12072. (b) Fu, G.; Xu, X.; Lu, X.; Wan, H. *J. Am. Chem. Soc.* **2005**, *127*, 3989. (c) Zhang, G.; Li, S.; Jiang, Y. *Organometallics* **2004**, *23*, 3656. (d) Rivalta, I.; Russo, N.; Sicilia, E. *J. Comput. Chem.* **2006**, *27*, 174.

(48) (a) Hogan, T.; Sen, A. *J. Am. Chem. Soc.* **1997**, *119*, 2642. (b) Lin, M.; Sen, A. *Chem. Commun.* **1992**, 892. (c) Basicckes, N.; Hogan, T. E.; Sen, A. *J. Am. Chem. Soc.* **1996**, *118*, 13111. (d) Sen, A. *Acc. Chem. Res.* **1998**, *31*, 550.

Scheme 1

Table 1. Conversion of Methane into Acetic Acid (Selected Data)^a

| entry ^b | catalyst | P_{CH_4} [atm] ^c | P_{CO} [atm] ^c | $n(\text{oxidant})/$ $n(\text{catalyst})$ | TON ^d | yield [%] ^e |
|----------------------|-----------|---|---------------------------------------|--|------------------|---------------------------|
| 1(12) ^f | 1 | 5 | 5 | 100 | 13.6 | 29.8 |
| 2(26) ^g | 1 | 5 | 5 | 250 | 19.3 | 42.2 |
| 3(32) ^{h,i} | 2 | 5 | 15 | 200 | 12.0 | 54.3 |
| 4(34) | 3 | 5 | 7.5 | 200 | 19.7 | 43.0 |
| 5(41) | 4 | 5 | 15 | 200 | 8.7 | 19.1 |
| 6(44) | 5 | 5 | 12.5 | 200 | 20.7 | 45.2 |
| 7(50) | 10 | 5 | 15 | 200 | 12.7 | 27.8 |

^a For more examples, see Table 1S (supporting data); reaction conditions (unless stated otherwise): metal complex catalyst (0.0625 mmol), K₂S₂O₈ (12.5 mmol, i.e., 200:1 molar ratio of oxidant to metal catalyst), CF₃COOH (23 mL), 80 °C, 20 h, in an autoclave (39 mL capacity); amounts of CH₄ or CO gases correspond to 0.575 mmol·atm⁻¹ with pressure measured at 25 °C. ^bNumber in parentheses corresponds to the entry number in the supplementary Table 1S. ^cMeasured at 25 °C. ^dTurnover number (mol of acetic acid per mol of metal catalyst) determined by GC or GC-MS. ^eMolar yield [%] based on CH₄, i.e., mol of acetic acid per 100 mol of methane; molar yields [%] based on K₂S₂O₈ (oxidant), if required, can be estimated as [TON × 100]/[$n(\text{oxidant})/n(\text{catalyst})$]. ^fTwo times less oxidant was used (6.25 mmol). ^gThe corresponding amount of (NH₄)₂S₂O₈ was used instead of K₂S₂O₈. ^hFrom ref 35. ⁱLess CH₄ was used (1.02 mmol) than that in the conditions described in footnote [a] by using a smaller reactor (23.5 mL).

2. Results and Discussion

The studies were undertaken by treatment of the metal catalyst, contained in a stainless steel autoclave, with a peroxo-oxidant, i.e., K₂S₂O₈ or (NH₄)₂S₂O₈, and the solvent, CF₃COOH (TFA), followed by flushing with N₂ for removal of the air, whereafter methane (and carbon monoxide when this gas was used) was (were) admitted to the required pressure(s). The system was then heated and magnetically stirred, and the final reaction solution was analyzed by gas chromatography (GC), GC-MS, and/or ¹³C and ¹H NMR.

Acetic acid was obtained (Scheme 1), and the source of its methyl group was proved to be methane as indicated by ¹³C-labeled experiments (see below). In fact, ¹³CH₃COOH, identified by ¹³C-¹H and ¹³C NMR spectroscopies, was formed either in the absence or in the presence of CO, when using labeled ¹³CH₄ as the substrate. In the former case, TFA was the carboxylating agent, but when the reaction was carried out in the presence of ¹³CO, this gas was also a carbonyl source as indicated by the formation of CH₃¹³COOH.

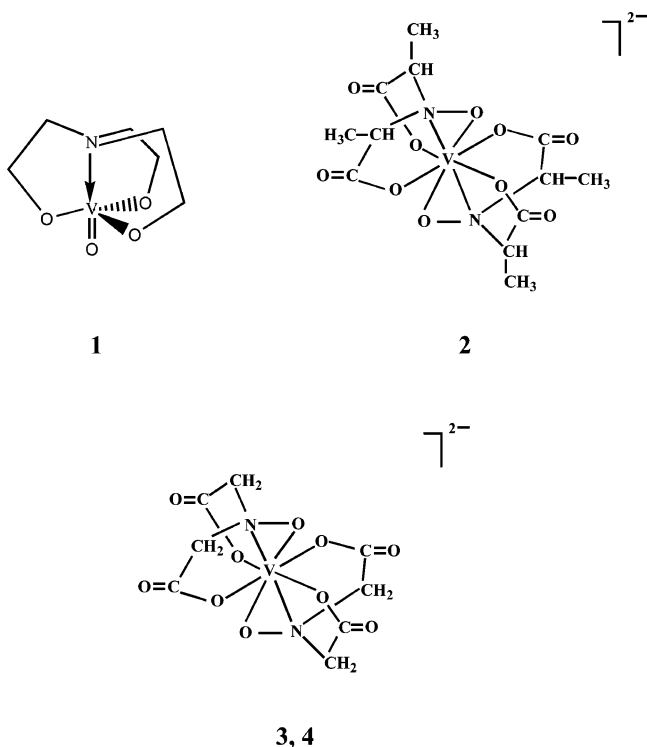
The effects of a variety of factors on the yield and TON were investigated in a systematic manner, and the results are summarized in Tables 1, 2, and 1S, for the following vanadium compounds used as catalyst precursors (for the abbreviations, see Experimental Section): [VO{N(CH₂CH₂O)₃}] **1**, Ca-[V(HIDPA)₂] **2** (synthetic *amavadin* as a racemic mixture), Ca[V(HIDA)₂] **3** and [Bu₄N]₂[V(HIDA)₂] **4** (*amavadin* models), [VO(CF₃SO₃)₂]·2H₂O **5**, Ba[VO(anta)(H₂O)]₂ **6**, [VO(ada)(H₂O)] **7**, [VO(Hheida)(H₂O)] **8**, [VO(bicine)] **9**, [VO(dipic)-

Table 2. Effect of Catalyst Amount^a

| entry | catalyst | $n(\text{CH}_4)/$ $n(\text{catalyst})$ | P_{CH_4} [atm] ^b | P_{CO} [atm] ^b | TON ^c | yield [%] ^d |
|-------|----------------------|---|---|---------------------------------------|------------------------|---------------------------|
| 1 | — | — | 5 | 0–15 | — | 0 |
| 2 | 2 | 46 | 5 | 0 | 13.4 | 29.4 |
| 3 | 2^e | 25.6 × 10 ³ | 5 | 0 | 3.72 × 10 ³ | 14.5 |
| 4 | 2 | 46 | 5 | 7.5 | 9.7 | 21.2 |
| 5 | 2^e | 25.6 × 10 ³ | 5 | 7.5 | 2.64 × 10 ³ | 10.3 |
| 6 | 3^e | 12.8 × 10 ³ | 5 | 15 | 1.82 × 10 ³ | 14.2 |
| 7 | 3^e | 12.8 × 10 ³ | 5 | 0 | 3.58 × 10 ³ | 28.0 |
| 8 | 3 | 46 | 5 | 7.5 | 19.7 | 43.0 |
| 9 | 3^e | 25.6 × 10 ³ | 5 | 7.5 | 5.39 × 10 ³ | 21.1 |
| 10 | 3 | 110 | 12 | 15 | 27.9 | 25.4 |
| 11 | 3^e | 25.6 × 10 ³ | 12 | 15 | 5.63 × 10 ³ | 8.8 |

^a Reaction conditions (unless stated otherwise): metal complex catalyst (20.00 μmol – 0.04 μmol), K₂S₂O₈ (4.2 mmol), CF₃COOH (7.3 mL), 80 °C, 20 h, in an autoclave (13 mL capacity). ^bAmounts of CH₄ or CO gases correspond to 0.213 mmol·atm⁻¹ with pressure measured at 25 °C. ^cTurnover number (mol of acetic acid per mol of metal catalyst); TOF (mol of acid/mol of catalyst per hour) can be estimated as TON/20 h⁻¹. ^dMolar yield [%] based on CH₄, i.e., mol of acetic acid per 100 mol of methane (determined by GC or GC-MS); molar yields [%] based on K₂S₂O₈, if required, can be estimated as 0.25 × yield (based on CH₄) for runs 1–9 (by taking into account that the CH₄/K₂S₂O₈ molar ratio is 0.25) or 0.61 × yield (based on CH₄) for runs 10–11 (by taking into account that the CH₄/K₂S₂O₈ molar ratio is 0.61). ^eMetal complex catalyst was used as an ultrafine mixture.

(OCH₂CH₃)] **10**, VOSO₄·5H₂O **11**, V₂O₄ **12**, and V₂O₅ **13**. Related complexes, with other metals, [PPh₄][Ta(HIDA)₂] **14**, [PPh₄][Nb(HIDA)₂] **15**, [PPh₄][Mo(HIDPA)₂] **16**, and [TaO-{N(CH₂CH₂O)₃}] **17**, have also been tested as catalysts, for comparative purposes. Blank tests indicate that no product formation was detected unless the catalyst was added.



The most active catalysts, **1–3** (or **4**), display triethanolamine or (hydroxyimino)dicarboxylates and can lead, in a single bath, to acetic acid yields up to 54% (based on CH₄, or 14% based on K₂S₂O₈) (Tables 1 and 1S) for a typical CH₄/V-catalyst molar ratio of 46. Remarkably TONs up to 5.6 × 10³ mol of CH₃COOH/mol of V-catalyst can be achieved when using

sufficiently low catalyst amounts (CH_4/V -catalyst molar ratio of 26×10^3) (Table 2).

2.1. Effect of the Reaction Time, Temperature, and Solvent. The reaction time to obtain the highest yield of acetic acid is dependent on the type of catalyst. Thus, in the case of complex **1** no product formation was detected within 0.5 h (Table 1S, entry 4), whereas, after 2 h, a *ca.* 20% yield of acetic acid (entry 5) was obtained. Extending the reaction time up to 20 h had no significant effect, leading to a yield of *ca.* 21% (Table 1S, entry 6). In contrast, the extension of the reaction time from 2 to 20 h, when complex **2** was used as the catalyst, resulted in a doubling of the yield from *ca.* 15 to *ca.* 29%, respectively (Table 1S, entries 28, 29). No loss of acid due to overoxidation to CO_2 was observed, since no appreciable yield drop was detected along the extended reaction time, for typical conditions. Moreover, by using acetic acid instead of methane, as a potential substrate, this acid is still present at the end of the experiment in a similar amount. Hence, further reactions were typically run for 20 h.

The temperature of 80 °C leads to the highest conversions, in accord with previous studies of methane carboxylation in $\text{K}_2\text{S}_2\text{O}_8/\text{TFA}$ using vanadium containing heteropolyacids³² and CaCl_2 ⁴⁹ catalysts.

Trifluoroacetic acid is a solvent applied in various alkane functionalization reactions,^{9,13,20–27,31,35,49,50} but its use still remains a drawback due to its significant cost. However, our attempts to fully substitute it for other more convenient solvents (water, ethanol, acetonitrile, dichloromethane, chloroform, formic acid, trichloroacetic acid, sulfuric acid, and Caro's acid {bearing H_2SO_5 , i.e., peroxymonosulfuric acid, a strong oxidant}) have failed.

2.2. Effect of Ligands, Counterion, and Metal Type of the Catalyst. The ligand type in the vanadium catalyst has a strong effect on the catalytic activity, and the most active systems are provided by complexes **1**, **2**, **3** (or **4**), with N,O-ligands corresponding to the basic forms of triethanolamine, 2,2'-(hydroxyimino)dipropionic, and 2,2'-(hydroxyimino)diacetic acids, respectively, which can lead to yields of acetic acid higher than 50% and/or TONs of about 30 (Tables 1 and 1S). A simple saltlike **11** ($\text{VOSO}_4 \cdot 5\text{H}_2\text{O}$), under the same reaction conditions, is much less active (Table 1S, entries 51 and 52) than the vanadium complexes **1–5** and **10** containing various N,O- or O,O-polydentate ligands. The relevance of N,O-type ligands or N-heterocyclic carboxylic acids cocatalysts has been recognized^{1,51} for other alkane oxidation systems, in assisting proton-transfer steps.

Once the calcium-catalyzed transformation of CH_4 and CO into acetic acid was reported,²² we have checked for a possible influence of the Ca^{2+} counterion in compound **3**, by comparing its activity with that of its *tetra*-butylammonium analogue **4**, under similar conditions. Identical yields were obtained (Table 1S, entries 35 and 41, respectively), indicating that the activity is not determined by the calcium counterion.

Since the vanadium complexes with N,O-ligands behave as the most active catalysts, the related complexes with metals of

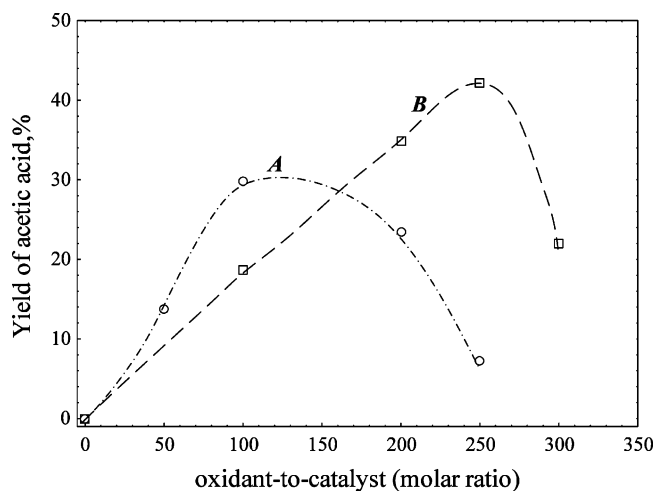


Figure 1. Effect of the oxidant and its amount on the yield of acetic acid using catalyst **1** and $\text{K}_2\text{S}_2\text{O}_8$ (**A**) or $(\text{NH}_4)_2\text{S}_2\text{O}_8$ (**B**) as the oxidant, for constant pressures (5 atm) of CH_4 and CO , at 80 °C in TFA.

groups V and VI [$\text{Ta}(\text{HIDA})_2$][−] **14**, [$\text{Nb}(\text{HIDA})_2$][−] **15**, [$\text{Mo}(\text{HIDPA})_2$][−] **16**, and [$\text{TaO}\{\text{N}(\text{CH}_2\text{CH}_2\text{O})_3\}$][−] **17** were also tested for comparison. The Ta (**14**) and Mo (**16**) complexes display a much lower activity (*ca.* 3% yield) than that the V analogues (Table 1S, entries 55 and 57), whereas the Nb (**15**) and Ta (**17**) compounds are fully inactive (entries 56 and 58).

Taking into account that the vanadium complexes **1**, **2**, and **3** are the best catalysts for the reaction, the impact of various factors on their activity, aiming at the optimization of conditions and getting information with mechanistic significance, was investigated in detail, as discussed below.

2.3. Effect of Catalyst Amount. A decrease in the amount of catalyst leads to a dramatic increase of TON, although with a reduction in product yield (see Table 2 for selected examples). For example, for *Amavadin* (**2**), an increase of the methane-to-catalyst molar ratio from 46:1 to 25.6×10^3 :1 results in TON and yield variations of 13.4 to 3.72×10^3 and 29.4% to 14.5%, respectively (Table 2, entries 2 and 3). An even higher TON enhancement to 5.63×10^3 is observed for the *Amavadin* model **3** (Table 2, entry 11), corresponding to a turnover frequency (TOF) of 282 mol of acetic acid/mol of V-catalyst per hour.

Such high TON values, which still correspond to considerably high yields (up to 28%) of acid, are quite remarkable in the field of functionalization of gaseous alkanes under mild conditions and have been achieved only very recently with other catalysts^{52a} or only for propane.^{52b}

However, the study of the other factors (besides the catalyst amount) has been undertaken with the more convenient higher amounts of vanadium catalyst (Table 1S) which are easier to handle and lead to higher yields and more pronounced variations that are easier to detect.

2.4. Effect of the Oxidant. Both the oxidant type and its relative amount have an effect on the yield of acetic acid, as shown in Figure 1 for catalyst **1** with constant pressures (5 atm) of CH_4 and CO . No reaction occurs in the absence of an oxidant. Potassium peroxodisulfate is the most effective one within the

(49) Asadullah, M.; Kitamura, T.; Fujiwara, Y. *J. Catal.* **2000**, *195*, 180.

(50) Yin, G.; Piao, D. G.; Kitamura, T.; Fujiwara, Y. *Appl. Organomet. Chem.* **2000**, *14*, 438.

(51) Shul'pin, G. B.; Kozlov, Yu. N.; Nizova, G. V.; Süß-Fink, G.; Stanislas, S.; Kitaygorodskiy, A.; Kulikova, V. S. *J. Chem. Soc., Perkin Trans.* **2001**, *2*, 1351.

(52) (a) Kirillova, M. V.; Kirillov, A. M.; Reis, P. M.; Silva, J. A. L.; Fraústo da Silva, J. J. R.; Pombeiro, A. J. L. *J. Catal.* **2007**, *248*, 130. (b) Kirillova, M. V.; da Silva, J. A. L.; Fraústo da Silva, J. J. R.; Palavra, A. F.; Pombeiro, A. J. L. *Adv. Synth. Catal.*, accepted for publication.

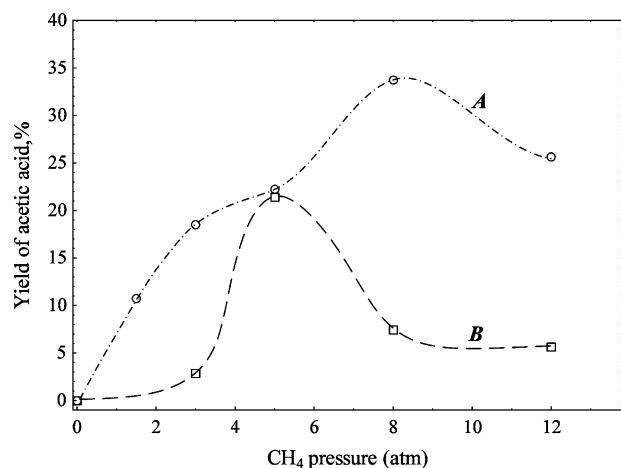


Figure 2. Effect of the CH₄ pressure on the yield of acetic acid using catalyst **1**. Reaction conditions: $n(\text{K}_2\text{S}_2\text{O}_8)/n(\text{catalyst}) = 200$, $P_{\text{CO}} = 15$ atm (curve **A**); $n(\text{K}_2\text{S}_2\text{O}_8)/n(\text{catalyst}) = 200$, $P_{\text{CO}} = 0$ atm (curve **B**).

0–150 range of the oxidant-to-catalyst molar ratio (Figure 1, curve **A**). The yield of acetic acid increases up to 30% on changing this ratio from 0 to 130, but a further enhancement of the amount of $\text{K}_2\text{S}_2\text{O}_8$ leads to a drop in yield conceivably due to poor stirring and the limited solubility of this compound. Moreover, subsequent oxidation of acetic acid, in the presence of a very high excess of $\text{K}_2\text{S}_2\text{O}_8$, cannot also be ruled out under these conditions. A high excess of this reagent also favors other reactions (see Scheme 5, route **C**) with a resulting decrease of acetic acid yield.

In the case of ammonium peroxodisulfate (Figure 1, curve **B**) the yield of acetic acid rises to 42% for a high oxidant-to-catalyst ratio (250), in accord with the slightly higher solubility of this oxidant in comparison with the potassium salt in TFA. A further increase in the amount of oxidant, as in the case of $\text{K}_2\text{S}_2\text{O}_8$, results in a marked yield drop, possibly for the reasons given above.

Other common oxidizing agents such as KMnO_4 , MnO_2 , $\text{K}_2\text{Cr}_2\text{O}_7$, H_2O_2 (30% in H_2O), and oxone ($2\text{KHSO}_5 \cdot \text{KHSO}_4 \cdot \text{K}_2\text{SO}_4$) were found to be inactive under the reaction conditions used.

2.5. Effect of Methane Pressure. The effect of the pressure of methane on the yield of acetic acid (for constant values of CO pressure and oxidant/catalyst ratio) in the reaction catalyzed by complex **1** is shown in Figure 2. In the presence of CO (curve **A**) the yield increases up to a methane pressure of 8 atm, beyond which it drops. The curve appears to result from the partial overlap of two other curves with maxima at *ca.* 3 and 8 atm, a feature that might be of mechanistic significance (see below). In the absence of CO the yield is very low for a low CH₄ pressure (0–2 atm) but increases sharply with this pressure up to 5 atm [*ca.* 21% (curve **B**) or 42% (curve **C**) for $\text{K}_2\text{S}_2\text{O}_8$, respectively], whereupon it decreases. Hence, the CH₄ pressure has to be chosen carefully, in particular when operating without CO (the optimum pressure is then 5 atm).

Similar types of dependences, with and without CO, appear to occur for the reaction catalyzed by complex **3** (Table 1S, entries 35, 38, 40, and 33, 36, 37, 39, respectively).

2.6. Effect of Carbon Monoxide Pressure. The effect of the CO pressure was studied for complexes **1**, **2**, and **3** as catalysts and $\text{K}_2\text{S}_2\text{O}_8$ (Figure 3) as oxidant. A relevant observation is that the systems are catalytic even in the absence of CO.

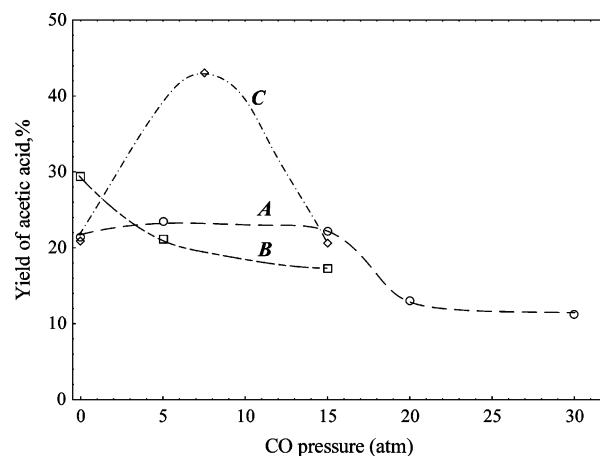


Figure 3. Effect of the CO pressure on the yield of acetic acid derived from methane (5 atm) using catalyst **1** (curve **A**), **2** (curve **B**), or **3** (curve **C**) and $\text{K}_2\text{S}_2\text{O}_8$ in TFA.

In particular, the activity of the system formed by complex **2** with $\text{K}_2\text{S}_2\text{O}_8$ (Figure 3, curve **B**) is maximum (30% yield) without CO, decreasing with an increase in pressure of this gas. For the complex **1**/ $\text{K}_2\text{S}_2\text{O}_8$ system (Figure 3, curve **A**), the activity is nearly constant (*ca.* 22% yield) until $P_{\text{CO}} = 15$ atm and higher CO pressures lead to an inhibiting effect.

For the other systems, the acetic acid yield increases with CO pressure until a maximum is reached, whereupon a further increase in pressure usually results in a lowering of the catalytic activity. For the complex **3**/ $\text{K}_2\text{S}_2\text{O}_8$ system (Figure 3, curve **C**) the optimum pressure is *ca.* 7 atm. Hence, in all cases there is no advantage in using a CO pressure above 7 atm, and the CO inhibiting effect observed in various cases for higher pressures presumably results from the formation of inactive carbonyl complexes.

In some of the systems there is an optimum CO pressure, but others operate better in the absence of CO (complex **2**/ $\text{K}_2\text{S}_2\text{O}_8$) or with an identical activity in the presence and in the absence of this gas (complex **1**/ $\text{K}_2\text{S}_2\text{O}_8$). Therefore, for such cases it would be advantageous to eliminate CO from the reaction system, making the system simpler while avoiding the use of a noxious reagent. The TFA solvent then acts as the carbonylating agent of methane, in the presence of the vanadium catalyst, a behavior that is in agreement with other reports.^{33,35} In particular, it has been shown³³ that TFA reacts with CH₄ in the presence of $[\text{VO}(\text{acac})_2]/\text{K}_2\text{S}_2\text{O}_8$, to yield acetic acid and CHF_3 via an unknown mechanism.

However, in the absence of CO, the methyl ester of TFA ($\text{CF}_3\text{COOCH}_3$) is also formed although usually in a lower yield in comparison with acetic acid. The presence of CO strongly inhibits the formation of this ester which is not detected at a P_{CO} of *ca.* 5 atm, the reaction proceeding with a high selectivity toward acetic acid formation.

Carbon dioxide is also formed during the reaction, carried out either in the presence or in the absence of CO. In the former case, the CO_2 yield is *ca.* 20% based on CO (under the conditions of run 38, but with $P_{\text{CH}_4} = 10$ atm, Table 1S), while, in the latter case (without using CO), it is only *ca.* 7%. Hence, both CO and TFA appear to be sources of CO_2 . The thermal decarboxylation of TFA, conceivably accelerated by the metal

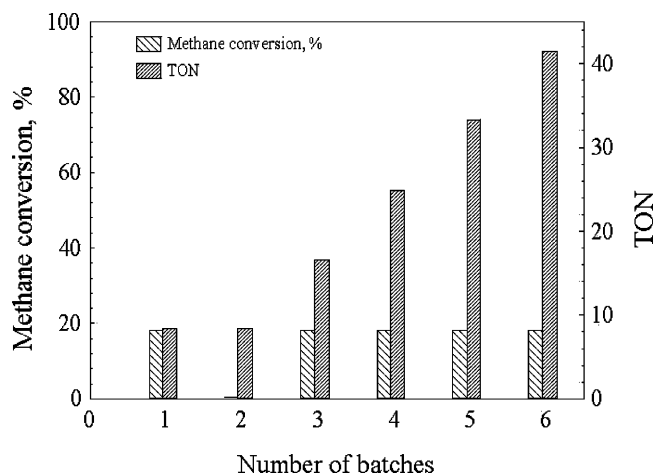


Figure 4. Methane carboxylation with multiple recycling (according to Scheme 1S) catalyzed by complex **1**/ $K_2S_2O_8$ (batch 2 was performed without addition of a new portion of $K_2S_2O_8$).

catalyst, to give CO_2 and CF_3H , is a known^{13,53} reaction. CO_2 is not believed to be derived from acetic acid since no appreciable overoxidation of this acid was detected (see above).

2.7. Multiple Recycling. We have tested the recycling of reagents and solvents with complex **1** in the presence of $K_2S_2O_8$, as follows (Supplementary Scheme 1S). Upon completion of each batch, a small aliquot of the reaction mixture was analyzed and the portion remaining in the reactor was used for the next batch, which was initiated by addition of CH_4 , CO , and usually $K_2S_2O_8$ (one run was performed without further addition of the oxidant, for comparative purposes).

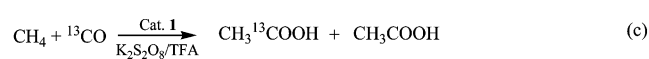
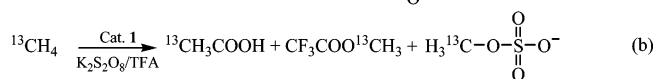
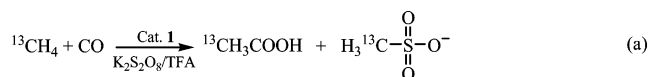
The first batch [performed under the conditions indicated in the Experimental Section, with CH_4 and CO pressures of 5 and 10 atm, respectively] afforded acetic acid with a yield of 18.4% and TON of 8.3 (Figure 4, batch 1). Repeating the experiment without the addition of new portions of both oxidant and catalyst (Figure 4, batch 2) did not lead to the formation of additional acetic acid. However, addition of a new portion of oxidant fully restores the activity of the system leading again to 18% conversion of fresh methane into acetic acid with a 2-fold enhancement of the TON (Figure 4, batch 3), without requiring any fresh catalyst. The catalyst, therefore, remains active. The procedure can be repeated, and after a total of five additions of oxidant (batch 6) the original level of activity of the catalyst is still preserved (i.e., methane conversion of ca. 18%) corresponding to a total TON value of ca. 42. After each batch, the addition of fresh oxidant is required for regenerating the activity of the system.

The efficacy of the recycling procedure is strongly dependent on the particular catalytic system. Hence, the complex **3**/ $K_2S_2O_8$ system remains active for only two recyclings.

2.8. ^{13}C -Labeled Experiments. In order to unambiguously establish the origin of the methyl and carbonyl groups in the acetic acid product, the reaction was studied in the presence of $^{13}CH_4$ or ^{13}CO and the ^{13}C -enriched products were clearly detected by ^{13}C NMR (Scheme 2).

The methyl or carbonyl groups of acetic acid were found to be enriched in ^{13}C when the reactions (a or c) were carried out in the presence of $^{13}CH_4$ or ^{13}CO , respectively, thus confirming

Scheme 2



that acetic acid originates from both methane and carbon monoxide. However, when the $^{13}CH_4$ reaction is performed in the absence of CO (reaction b), the source of the carbonyl group is not methane (no ^{13}C enriched carbonyl group was detected), thus indicating that TFA plays such a role. In the reaction of unlabeled methane with ^{13}CO (reaction c), $CH_3^{13}COOH$ is also formed (the $CH_3^{13}COOH/CH_3COOH$ ratio is 1.5), thus clearly indicating the involvement of two pathways for acetic acid formation, i.e., (i) methane carbonylation by ^{13}CO (the more preferable one, even at the low ^{13}CO pressure of 2 atm) and (ii) carbonylation by CF_3COOH .

The formation of methanesulfonate in reaction a and methyl sulfate in b is also observed at the low $^{13}CH_4$ pressure used (below 2 atm), but these products are not formed under the usual reaction conditions (higher methane pressures). The methyl trifluoroacetate ester is formed in the absence of CO (reaction b) in lower yield than acetic acid.

2.9. Proposed Mechanism. In this section, on the basis of some experimental results and DFT calculations, we discuss plausible mechanisms of carboxylation of methane by the peroxodisulfate/TFA system, which had not been previously the object of a theoretical study.

Although the involvement of radical species in our systems has been demonstrated and the methyl radical was trapped (see below), attempts to isolate and fully characterize any intermediate metal complex have not yet been successful. However, initial oxidation to V^V by the peroxide occurs when using a starting V^{IV} compound in accord with the known oxidation,^{54,55} by a peroxide, of the blue vanadium(IV) species **2–4** to the corresponding deep red vanadium(V) complexes.

Moreover the key role played by a peroxo-vanadium(V) complex, derived from peroxidation of an oxo-vanadium(V) species (replacement of an oxo by a peroxo ligand), has been recognized in the mechanism of peroxidative halogenation reactions catalyzed by vanadium haloperoxidases,^{56a} and a number of peroxo-vanadium(V) complexes have been reported and applied as models.^{56–58} Hence, in view of the similarity of

(54) Reis, P. M.; Silva, J. A. L.; Fraústo da Silva, J. J. R.; Pombeiro, A. J. L. *Chem. Commun.* **2000**, 1845.

(55) Matoso, C. M. M.; Pombeiro, A. J. L.; Fraústo da Silva, J. J. R.; Guedes da Silva, M. F. C.; da Silva, J. A. L.; Baptista-Ferreira, J. L.; Pinho-Almeida, F. In *Vanadium Compounds - Chemistry, Biochemistry and Therapeutic Applications*; Tracey, A. C., Crans, D. C., Eds.; American Chemical Society Symposium Series, no. 711: Oxford University Press, 1998; Chapter 18, p 241.

(56) Various chapters in *Vanadium Compounds - Chemistry, Biochemistry and Therapeutic Applications*; Tracey, A. C., Crans, D. C., Eds.; American Chemical Society Symposium Series, no. 711: Oxford University Press, 1998: (a) Pecoraro, V. L.; Sleboznick, C.; Hamstra, B. Chapter 12, p 157. (b) Crans, D. C.; Tracey, A. S. Chapter 1, p 2. (c) Rehder, D.; Bashirpoor, M.; Jantzen, S.; Schmidt, H.; Farahbakhsh, M.; Nekola, H. Chapter 4, p 60. (d) Schwendt, P.; Sivák, M. Chapter 8, p 117. (e) Conte, V.; Di Furia, F.; Moro, S. Chapter 10, p 136. (f) Messerschmidt, A.; Prade, L.; Wever, R. Chapter 14, p 186. (g) Butler, A.; Tschirret-Guth, R. A.; Simpson, M. T. Chapter 15, p 202.

(57) Crans, D. C.; Smees, J. J.; Gaidamauskas, E.; Yang, L. Q. *Chem. Rev.* **2004**, *104*, 849.

(53) Ashworth, A.; Harrison, P. G. *J. Chem. Soc., Faraday Trans.* **1993**, *89*, 2409.

some of our complexes, namely [VO{N(CH₂CH₂O)₃}] **1**, with the active center of those enzymes based on the vanadate core with one N-ligated imidazol of an histidine residue, the involvement, in our system, of a peroxo-vanadium(V) complex, e.g., [V(OO){N(CH₂CH₂O)₃}], or a related species is a reasonable proposal (see discussion below). In this respect, it is noteworthy to mention that the hydroxyimine(1-) group, η²-(O-N<), of the HIDPA³⁻ and HIDA³⁻ ligands is isoelectronic with peroxide(2-), and thus the oxidized forms of complexes **2–4** relate to di(peroxo)-vanadium(V) species.

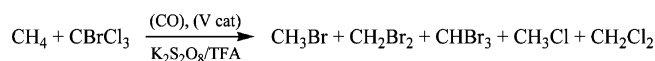
Although the starting complexes can, in principle, undergo displacement reactions with the solvent or oxidant, in the reaction medium, quantum chemical calculations on the system **1**/TFA/H₂O₂ (H₂O₂ was taken as the oxidant instead of K₂S₂O₈, for simplicity) indicate that **1** is thermodynamically more stable than possible products of partial or complete ethanolamine substitution (see Table 2S, Supporting Information). Moreover, the reaction of **1** with H₂O₂ involving H-transfer to the N,O-ligand to give [V(O)(OO){N(CH₂CH₂O)₂(CH₂CH₂OH)}]⁻ (reactions 21–23, Table 2S), similar to the first steps of a recently studied⁵⁹ mechanism of alkane oxidation, is also thermodynamically unfavorable. Thus, in the following mechanistic discussion, we consider the triethanolamine ligand is preserved in the active form of the catalyst derived from **1**.

2.9.1. Radicals Formation. Two main general types of mechanisms for the methane C–H bond activation can be considered,^{12,13} *a priori*: (i) a radical one, involving the homolytic cleavage of a C–H bond, and (ii) a non-radical one, proceeding via heterolytic C–H bond cleavage (CH₃⁻ abstraction with H⁺ loss) upon electrophilic attack of the metal center to that bond. The oxidative addition of methane (to give an hydride-methyl species) and the σ-bond metathesis (to form a methyl complex) are ruled out by the d⁰ electronic nature of vanadium(V) or the lack of a suitable σ-bonded ligand for the metathesis, respectively.

The radical route (i) is the one we believe to be followed in our cases, either in the presence or in the absence of CO, since the formation of acetic acid is hampered by undertaking the reaction in the presence of 2,6-di-*tert*-butyl-4-methylphenol (BHT), Ph₂NH, 5,5-dimethyl-1-pyrroline *N*-oxide, CBrCl₃, or even O₂, i.e., known^{48a,60} C- and/or O-centered radical traps. For example, no acid at all is formed (or only traces are detected) when using a stoichiometric (or a higher) amount of BHT relatively to CH₄ or an even lower relative amount of the pyrroline *N*-oxide compound, either in the absence or in the presence of CO (e.g., 0 or 15 atm) and at different methane pressures (e.g., 5 or 8 atm). Similarly, the presence of gaseous O₂ (1 atm) also results in a strong inhibiting effect on the formation of acetic acid. The final reaction mixture in the experiments with the pyrroline *N*-oxide species was EPR silent due to further decomposition under our reaction conditions.

When the carboxylation reaction was performed under the optimized conditions, either in the presence or in the absence of CO, but with added CBrCl₃ in the stoichiometric amount relatively to methane (Scheme 3), mono-, di-, and tribro-

Scheme 3



momethane, as well as CH₃Cl and CH₂Cl₂, were detected by ¹H and ¹³C NMR as the main products with an overall yield that is 7 times that of acetic acid. This observation with those discussed below provide strong evidence for the *formation of CH₃[•] which was trapped by CBrCl₃*. Acetic acid was revealed only in a small amount (yield below 2%).

For checking the eventual roles of vanadium and/or K₂S₂O₈ in the generation of the free radicals, the carboxylation reaction was rerun in the presence of a radical trap (under the above reaction conditions), but in the absence of the V-catalyst. In this case, trapping of the methyl radical was also observed by formation of the same haloalkanes, indicating that *vanadium was not required for CH₃[•] formation*. When the reaction was carried out in the presence of a V-catalyst and CBrCl₃, but in the absence of K₂S₂O₈, no products (neither halomethane derivatives nor acetic acid) were detected by ¹H and ¹³C NMR, which reveals the *determinant role of the peroxide in the radical formation*. In accord, the conditions are highly favorable for the formation of radicals from this peroxide. Hence, S₂O₈²⁻ or the protonated form HS₂O₈⁻ which is predominant in the acidic CF₃COOH medium can generate, upon known thermal decomposition,^{8,22,61} the sulfate and hydrosulfate radicals (SO₄^{•-} or HSO₄[•]) which are H-abstractors from alkanes.^{8,48b–d,50,62}

The quantum chemical calculations of the OO bond dissociation enthalpy in solution (ΔH_s) for HS₂O₈⁻ give a value of only 24.31 kcal/mol (at the B3LYP/6-311+G** levels of theory, reaction 1, Table 3), which is consistent with the bond dissociation enthalpies obtained experimentally for H₂S₂O₈ (22 kcal/mol⁶³) and S₂O₈²⁻ (29 kcal/mol⁶⁴). The entropic contribution should favor the decomposition of HS₂O₈⁻, and the calculated ΔG_s value is 9.60 kcal/mol, although it is underestimated due to the error in the entropic term (see Computational Details). It is worthwhile to note that the HSO₄[•] and SO₄^{•-} radicals are also formed when HS₂O₈⁻ (or S₂O₈²⁻) acts as a single-electron oxidant, e.g., of a V^{IV} species (see below, reaction 32 in Table 3).

Homolytic cleavage of a methane C–H bond by any of those peroxo-derived radicals could yield the methyl radical (Scheme 4, reactions 2a and 2b). For these processes, the transition states (TSs) corresponding to the hydrogen transfer from CH₄ to HSO₄[•] (**TS1a**) or to SO₄^{•-} (**TS1b**) (Figure 5) were located on the potential energy surface (PES). Examination of the energies of these TSs shows that (i) the reactions display rather low activation barriers (within 11 kcal/mol in terms of activation enthalpies in solution ΔH_s[‡]); (ii) the hydrosulfate radical HSO₄[•] is more reactive toward CH₄ by 7.12 kcal/mol, in comparison with SO₄^{•-}; and (iii) the formation of the CH₃[•] radical is exothermic and exoergonic, clearly in the case of the reaction 2a of HSO₄[•] and slightly for the reaction 2b of SO₄^{•-}. The formation of hydrogenosulfate HSO₄⁻ (reaction 2b) is proven

(58) Rehder, D.; Santoni, G.; Licini, G. M.; Schulzke, C.; Meier, B. *Coord. Chem. Rev.* **2003**, *237*, 53.

(59) Khaliullin, R. Z.; Bell, A. T.; Head-Gordon, M. *J. Phys. Chem. B* **2005**, *109*, 17984.

(60) (a) Slaughter, L. M.; Collman, J. P.; Eberspacher, T. A.; Brauman, J. I. *Inorg. Chem.* **2004**, *43*, 5198. (b) Cook, G. K.; Mayer, J. M. *J. Am. Chem. Soc.* **1994**, *116*, 1855.

(61) (a) Minisci, F.; Citterio, A. *Acc. Chem. Res.* **1983**, *16*, 27. (b) Walling, C.; Camaioni, D. M. *J. Am. Chem. Soc.* **1975**, *97*, 1603. (c) Walling, C.; Camaioni, D. M.; Kim, S. S. *J. Am. Chem. Soc.* **1978**, *100*, 4814. (d) Effenberger, F.; Kottmann, H. *Tetrahedron* **1985**, *41*, 4171.

(62) Huie, R. E.; Clifton, C. L. *Int. J. Chem. Kinet.* **1989**, *21*, 611.

(63) Benson, S. W. *Chem. Rev.* **1978**, *78*, 23.

(64) Brusa, M. A.; Churio, M. S.; Grella, M. A.; Bertolotti, S. G.; Previtali, C. *M. Phys. Chem. Chem. Phys.* **2000**, *2*, 2383.

Table 3. Energetic Characteristics (in kcal/mol) of the Reactions Involved in the Proposed Mechanisms for the CPCM-B3LYP/6-31+G**//gas-B3LYP/6-31G* and CPCM-B3LYP/6-31+G**//gas-B3LYP/6-31+G** (in Parentheses) Levels of Theory^a

| no. | reaction | ΔH_s^\ddagger | ΔH_s | ΔG_s |
|-----|---|-----------------------|--------------------------|-----------------|
| 1 | $\text{HS}_2\text{O}_8^- \rightarrow \text{HSO}_4^- + \text{SO}_4^{\cdot-}$ | | +24.86 (+24.31) | |
| 2a | $\text{HSO}_4^{\cdot-} + \text{CH}_4 \rightarrow \text{H}_2\text{SO}_4 + \text{CH}_3^{\cdot}$ | (via TS1a) | 5.06 (3.64) | -3.38 (-6.80) |
| 2b | $\text{SO}_4^{\cdot-} + \text{CH}_4 \rightarrow \text{HSO}_4^- + \text{CH}_3^{\cdot}$ | (via TS1b) | 7.60 (10.76) | +3.47 (-0.93) |
| 3 | $\text{CH}_4 + [\text{VO}\{\text{N}(\text{CH}_2\text{CH}_2\text{O})_3\}] \rightarrow \text{CH}_3^{\cdot} + [\text{V}(\text{OH})\{\text{N}(\text{CH}_2\text{CH}_2\text{O})_3\}]$ | | +42.22 | +40.03 |
| 4 | $\text{CH}_4 + [\text{V}(\text{OO})\{\text{N}(\text{CH}_2\text{CH}_2\text{O})_3\}] \rightarrow \text{CH}_3^{\cdot} + [\text{V}(\text{OOH})\{\text{N}(\text{CH}_2\text{CH}_2\text{O})_3\}]$ | | +34.61 | +31.46 |
| 5 | $\text{CH}_4 + [\text{VO}\{\text{N}(\text{CH}_2\text{CH}_2\text{O})_3\}] \rightarrow [\text{V}(\text{OH})(\text{CH}_3)\{\text{N}(\text{CH}_2\text{CH}_2\text{O})_3\}]$ | | +52.33 | |
| 6 | $\text{CH}_3^{\cdot} + \text{CO} \rightarrow \text{CH}_3\text{CO}^{\cdot}$ | (via TS2) | 2.86 (3.40) | -17.81 (-16.25) |
| 7a | $\text{HS}_2\text{O}_8^- + \text{CF}_3\text{COOH} \rightarrow \text{H}_2\text{SO}_5 + \text{CF}_3\text{C}(\text{O})\text{OSO}_3^-$ | | 30.96 (28.39) | +7.66 (+7.59) |
| 7b | $[\text{VO}\{\text{N}(\text{CH}_2\text{CH}_2\text{O})_3\}] + \text{H}_2\text{SO}_5 \rightarrow [\text{V}(\text{OO})\{\text{N}(\text{CH}_2\text{CH}_2\text{O})_3\}] + \text{H}_2\text{SO}_4$ | | +2.49 | +2.60 |
| 7c | $[\text{VO}\{\text{N}(\text{CH}_2\text{CH}_2\text{O})_3\}] + \text{HS}_2\text{O}_8^- \rightarrow [\text{V}(\text{OO})\{\text{N}(\text{CH}_2\text{CH}_2\text{O})_3\}] + \text{HS}_2\text{O}_7^-$ | | +8.16 | +7.88 |
| 8a | $[\text{V}(\text{OO})\{\text{N}(\text{CH}_2\text{CH}_2\text{O})_3\}] + \text{CH}_3\text{CO}^{\cdot} \rightarrow [\text{V}\{\text{OOC}(\text{O})\text{CH}_3\}\{\text{N}(\text{CH}_2\text{CH}_2\text{O})_3\}]$ | (via TS3a) | 4.39 | -58.10 |
| 8b | $[\text{V}\{\text{OOC}(\text{O})\text{CH}_3\}\{\text{N}(\text{CH}_2\text{CH}_2\text{O})_3\}] \rightarrow [\text{VO}\{\text{N}(\text{CH}_2\text{CH}_2\text{O})_3\}] + \text{CH}_3\text{COO}^{\cdot}$ | (via TS3b) | 5.98 ^b | -15.62 |
| 9 | $\text{CH}_3\text{COO}^{\cdot} + \text{CF}_3\text{COOH} \rightarrow \text{CH}_3\text{COOH} + \text{CF}_3\text{COO}^{\cdot}$ | (via TS4) | 2.08 (1.82) | +7.75 (+8.00) |
| 10 | $\text{CH}_3\text{COO}^{\cdot} + \text{CH}_4 \rightarrow \text{CH}_3\text{COOH} + \text{CH}_3^{\cdot}$ | (via TS5) | 10.45 (9.10) | +0.32 (-2.77) |
| 11 | $[\text{V}(\text{OO})\{\text{N}(\text{CH}_2\text{CH}_2\text{O})_3\}] + \text{CF}_3\text{COOH} \rightarrow [\text{V}(\text{OOH})\{\text{N}(\text{CH}_2\text{CH}_2\text{O})_3\}] + \text{CF}_3\text{COO}^{\cdot}$ | | +9.13 | +8.26 |
| 12 | $[\text{V}(\text{OOH})\{\text{N}(\text{CH}_2\text{CH}_2\text{O})_3\}] + \text{CH}_3\text{CO}^{\cdot} \rightarrow [\text{V}(\text{OOH})\{\text{N}(\text{CH}_2\text{CH}_2\text{O})_3\}] + \text{CH}_3\text{CO}^+$ | | -10.88 | -11.10 |
| 13 | $\text{CH}_3\text{CO}^+ + \text{CF}_3\text{COO}^- \rightarrow \text{CF}_3\text{C}(\text{O})\text{OC}(\text{O})\text{CH}_3$ | | -40.89 (-38.03) | |
| 14 | $\text{CH}_3\text{CO}^+ + \text{HSO}_4^- \rightarrow \text{CH}_3\text{C}(\text{O})\text{OSO}_2\text{OH}$ | | -36.88 (-33.13) | |
| 15 | $\text{CH}_3\text{CO}^+ + \text{SO}_4^{\cdot-} \rightarrow \text{CH}_3\text{C}(\text{O})\text{OSO}_3^{\cdot}$ | | -30.09 (-27.51) | |
| 16 | $\text{CH}_3\text{C}(\text{O})\text{OSO}_3^{\cdot} + \text{CH}_4 \rightarrow \text{CH}_3\text{C}(\text{O})\text{OSO}_2\text{OH} + \text{CH}_3^{\cdot}$ | (via TS6) | 3.22 (2.84) | -3.30 (-6.56) |
| 17a | $\text{HS}_2\text{O}_8^- + \text{CH}_3\text{CO}^{\cdot} \rightarrow \text{HSO}_4^{\cdot-} + \text{CH}_3\text{C}(\text{O})\text{OSO}_3^-$ | (via TS7a) | 6.51 (5.24) | -55.78 (-56.34) |
| 17b | $\text{HS}_2\text{O}_8^- + \text{CH}_3\text{CO}^{\cdot} \rightarrow \text{SO}_4^{\cdot-} + \text{CH}_3\text{C}(\text{O})\text{OSO}_2\text{OH}$ | (via TS7b) | 5.35 (4.60) | -57.92 (-58.25) |
| 18 | $\text{CH}_3\text{C}(\text{O})\text{OSO}_3^- + \text{CF}_3\text{COOH} \rightarrow \text{CH}_3\text{C}(\text{O})\text{OSO}_2\text{OH} + \text{CF}_3\text{COO}^-$ | | +11.44 (+11.58) | +10.56 (+10.66) |
| 19a | $\text{CF}_3\text{C}(\text{O})\text{OC}(\text{O})\text{CH}_3 + \text{CF}_3\text{COOH} \rightarrow \text{CF}_3\text{C}(\text{O})\text{OC}(\text{O})\text{CF}_3 + \text{CH}_3\text{COOH}$ | (via TS8a) | 27.09 (26.87) | +5.43 (+5.86) |
| | | (via TS8b) | 33.47 (32.70) | +5.51 (+5.56) |
| | | (via TS8c) | 37.04 (33.46) | |
| | | (via TS8d) | 51.78 (47.21) | |
| 19b | $\text{CF}_3\text{C}(\text{O})\text{OC}(\text{O})\text{CH}_3 + \text{CF}_3\text{COOH} \rightarrow \text{CF}_3\text{C}(\text{O})\text{OC}(\text{OH})\text{CH}_3^+ + \text{CF}_3\text{COO}^-$ | | +41.36 (+41.14) | +39.08 (+41.64) |
| 20 | $\text{CH}_3\text{C}(\text{O})\text{OSO}_3^- \rightarrow \text{CH}_3\text{COO}^- + \text{SO}_3$ | | +34.10 (+33.05) | |
| 21 | $\text{CH}_3\text{C}(\text{O})\text{OSO}_2\text{OH} \rightarrow \text{CH}_3\text{COO}^- + \text{HOSO}_2^+$ | | +95.42 (+94.47) | |
| 22 | $\text{CH}_3\text{C}(\text{O})\text{OSO}_2\text{OH} \rightarrow \text{CH}_3\text{COOH} + \text{SO}_3$ | (via TS9) | 0.76 (0.60) ^c | -1.76 (-0.06) |
| 23 | $\text{CH}_3\text{COOH} + \text{SO}_3 \rightarrow \text{CH}_3\text{COOH} + \text{SO}_3$ | | +9.70 (+7.16) | |
| 24a | $\text{CH}_3\text{C}(\text{O})\text{OSO}_2\text{OH} + \text{CF}_3\text{COOH} \rightarrow \text{CF}_3\text{C}(\text{O})\text{OC}(\text{O})\text{CH}_3 + \text{H}_2\text{SO}_4$ | (via TS10a) | 22.21 (15.50) | +2.69 (+2.72) |
| | | (via TS10b) | 32.36 (19.35) | +1.36 (+1.59) |
| 24b | $\text{CH}_3\text{C}(\text{O})\text{OSO}_2\text{OH} + \text{CF}_3\text{COOH} \rightarrow \text{CH}_3\text{COOH} + \text{CF}_3\text{COOH} + \text{SO}_3$ | (via TS11) | 28.20 (26.20) | +7.94 (+7.10) |
| 24c | $\text{CH}_3\text{C}(\text{O})\text{OSO}_2\text{OH} + \text{CF}_3\text{COOH} \rightarrow \text{CH}_3\text{COOH} + \text{CF}_3\text{C}(\text{O})\text{OSO}_2\text{OH}$ | (via TS12) | 48.22 (46.22) | +6.02 (+5.67) |
| 24d | $\text{CH}_3\text{C}(\text{O})\text{OSO}_2\text{OH} + \text{CF}_3\text{COOH} \rightarrow \text{CH}_3\text{C}(\text{OH})\text{OH} + \text{SO}_3 + \text{CF}_3\text{COO}^-$ | | +37.67 (+37.88) | +29.88 (+30.88) |
| 24e | $\text{CH}_3\text{C}(\text{O})\text{OSO}_2\text{OH} + \text{CF}_3\text{COOH} \rightarrow \text{CH}_3\text{COOH} + \text{SO}_2\text{OH}^+ + \text{CF}_3\text{COO}^-$ | | +36.52 (+37.72) | +34.07 (+35.50) |
| 25 | $\text{CH}_3^{\cdot} + \text{CF}_3\text{COOH} \rightarrow \text{CH}_4 + \text{CF}_3\text{COO}^{\cdot}$ | (via TS13) | 9.87 (13.22) | +7.45 (+10.77) |
| 26 | $\text{HSO}_4^{\cdot-} + \text{CF}_3\text{COOH} \rightarrow \text{H}_2\text{SO}_4 + \text{CF}_3\text{COO}^{\cdot}$ | (via TS14) | 13.32 (12.85) | +4.05 (+3.96) |
| 27 | $\text{CH}_3^{\cdot} + \text{CF}_3\text{COOH} \rightarrow \text{H}^{\cdot} + \text{CF}_3\text{COOCH}_3$ | | +23.58 (+28.60) | +28.22 (+33.26) |
| 28 | $\text{CH}_3^{\cdot} + \text{CF}_3\text{COO}^{\cdot} \rightarrow \text{CF}_3\text{COOCH}_3$ | | -87.37 (-86.57) | |
| 29 | $[\text{V}(\text{OOH})\{\text{N}(\text{CH}_2\text{CH}_2\text{O})_3\}] + \text{CH}_3^{\cdot} \rightarrow [\text{V}(\text{OOH})\{\text{N}(\text{CH}_2\text{CH}_2\text{O})_3\}] + \text{CH}_3^+$ | | +32.81 | +31.90 |
| 30a | $\text{HS}_2\text{O}_8^- + \text{CH}_3^{\cdot} \rightarrow \text{HSO}_4^{\cdot-} + \text{CH}_3\text{OSO}_3^-$ | (via TS15a) | 7.77 (7.54) | -50.03 (-50.46) |
| 30b | $\text{HS}_2\text{O}_8^- + \text{CH}_3^{\cdot} \rightarrow \text{SO}_4^{\cdot-} + \text{CH}_3\text{OSO}_2\text{OH}$ | (via TS15b) | 7.76 (7.80) | -56.64 (-56.61) |
| 31 | $\text{CH}_3\text{OSO}_3^- + \text{CF}_3\text{COOH} \rightarrow \text{CH}_3\text{OSO}_2\text{OH} + \text{CF}_3\text{COO}^-$ | | +6.97 (+7.34) | +5.23 (+5.66) |
| 32 | $[\text{V}(\text{OOH})\{\text{N}(\text{CH}_2\text{CH}_2\text{O})_3\}] + \text{HS}_2\text{O}_8^- \rightarrow [\text{V}(\text{OO})\{\text{N}(\text{CH}_2\text{CH}_2\text{O})_3\}] + \text{HSO}_4^- + \text{HSO}_4^{\cdot-}$ | | -5.73 | |

^a ΔG_s values are indicated only for the reactions which preserve the total number of molecules. ^b ΔG_s^\ddagger value is 3.91 kcal/mol. ^c ΔG_s^\ddagger values are 0.85 (0.97) kcal/mol.

by the isolation, in a good amount, of the KHSO_4 salt, from the final reaction mixture.

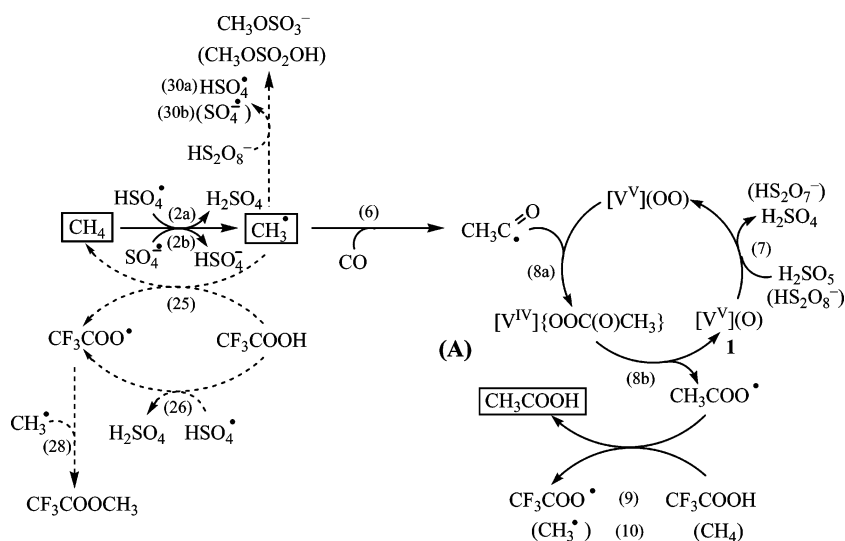
Alternative routes for the formation of CH_3^{\cdot} by methane reactions with an oxo- or peroxy-vanadium complex are thermodynamically quite unfavorable. Indeed, the homolytic H-atom abstraction from methane by $[\text{VO}\{\text{N}(\text{CH}_2\text{CH}_2\text{O})_3\}]$ **1** or $[\text{V}(\text{OO})\{\text{N}(\text{CH}_2\text{CH}_2\text{O})_3\}]$ to produce $[\text{V}(\text{OH})\{\text{N}(\text{CH}_2\text{CH}_2\text{O})_3\}]$ or $[\text{V}(\text{OOH})\{\text{N}(\text{CH}_2\text{CH}_2\text{O})_3\}]$ exhibits a ΔH_s value of +42.22 or +34.61 kcal/mol (at B3LYP/6-31G*), respectively (reactions 3 and 4, Table 3). Similarly, the heterolytic methane C-H bond cleavage in the reaction of CH_4 with **1** to form the methyl complex $[\text{V}(\text{OH})(\text{CH}_3)\{\text{N}(\text{CH}_2\text{CH}_2\text{O})_3\}]$ displays $\Delta H_s = +52.33$ kcal/mol (reaction 5). Therefore, such V-assisted routes were discarded.

2.9.2. Carbonylation. The formed CH_3^{\cdot} radical easily undergoes exothermic carbonylation by CO to afford the acyl $\text{CH}_3\text{CO}^{\cdot}$ radical (reaction 6) *via* the “early” transition state **TS2** (Figure 5) with a low activation barrier (ΔH_s^\ddagger of 3.40 kcal/mol). In the absence of CO, the carbonyl group of $^{13}\text{CH}_3\text{COOH}$ (derived from $^{13}\text{CH}_4$) must originate from the solvent $\text{CF}_3\text{-COOH}$. This process was described by Bell et al.,³³ and the

proposed mechanism involves thermolytic cleavage of the OO bond of peroxydisulfate, H-abstraction from CH_4 by the sulfate radical, and formation of $\text{CH}_3\text{COO}^{\cdot}$ upon reaction of CH_3^{\cdot} with CO_2 , the latter being produced by oxidation of TFA.^{9,13,22,25,50,65} Since the last reaction ($\text{CH}_3^{\cdot} + \text{CO}_2$) is endothermic ($\Delta H_s = +7.54$ kcal/mol at CPCM-B3LYP/6-31+G**), the role of the catalyst could consist of stabilization of reaction products.³³ Another product of the overall reaction ($\text{CH}_4 + \text{CF}_3\text{COOH} \rightarrow \text{CH}_3\text{COOH} + \text{CF}_3\text{H}$), i.e., trifluoromethane CF_3H ,³³ was not detected in our system in the liquid phase, but its presence in the gas phase was suggested by its characteristic IR band at 1166 cm^{-1} . Alternatively, it was proposed⁶⁵ that the reaction of CH_3^{\cdot} with CF_3COOH would lead to the acyl radical $\text{CH}_3\text{-CO}^{\cdot}$ and CF_3OH that would decompose to COF_2 and HF. However we were unable to calculate any reaction pathway with a reasonably low activation barrier leading to CF_3OH or HF.

2.9.3. Further Conversions of $\text{CH}_3\text{CO}^{\cdot}$. Three further reactions of $\text{CH}_3\text{CO}^{\cdot}$ were considered, i.e., (A) the oxygenation of $\text{CH}_3\text{CO}^{\cdot}$ with the peroxy-complex $[\text{V}(\text{OO})\{\text{N}(\text{CH}_2\text{CH}_2\text{O})_3\}]$

(65) Gekhman, A. E.; Moiseeva, N. I.; Moiseev, I. I. *Russ. Chem. Bull.* **1995**, *44*, 584.

Scheme 4. Proposed Mechanisms for Radical Formation and Carboxylation of Methane to Acetic Acid [Route (A)] and Side Reactions (Dotted Lines)^a

^a Reaction numbers correspond to those of Table 3. [V] = vanadium metal center namely V{N(CH₂CH₂O)₃}.

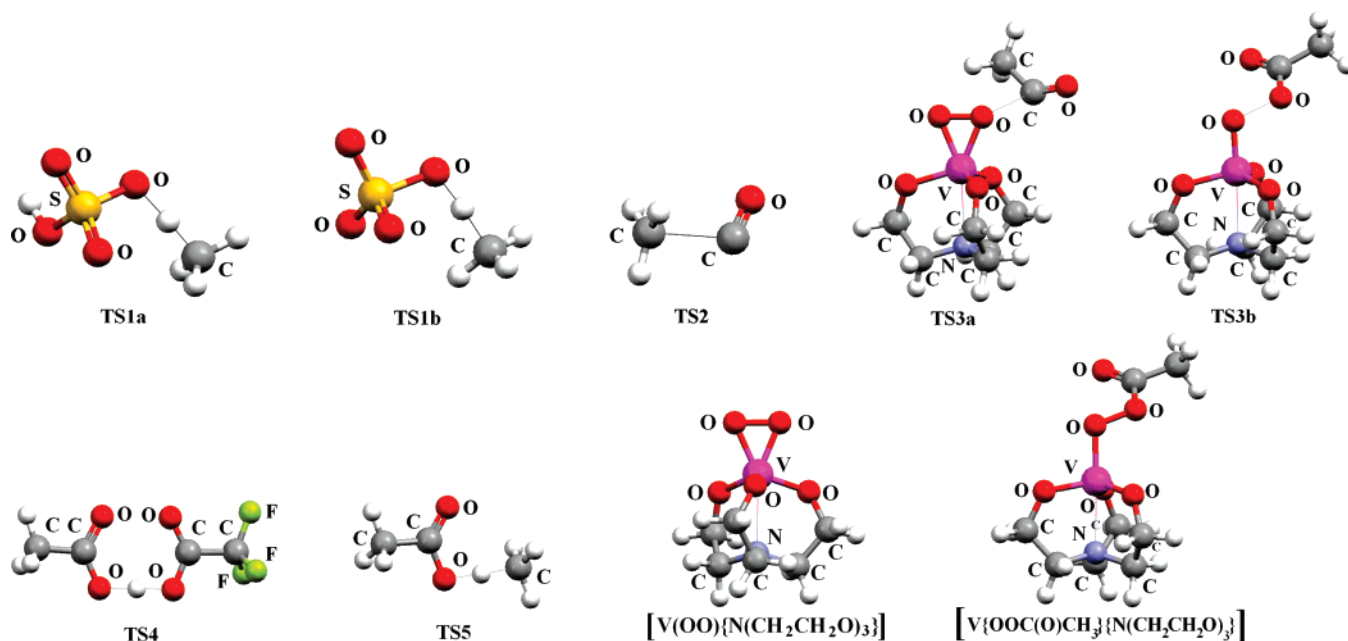


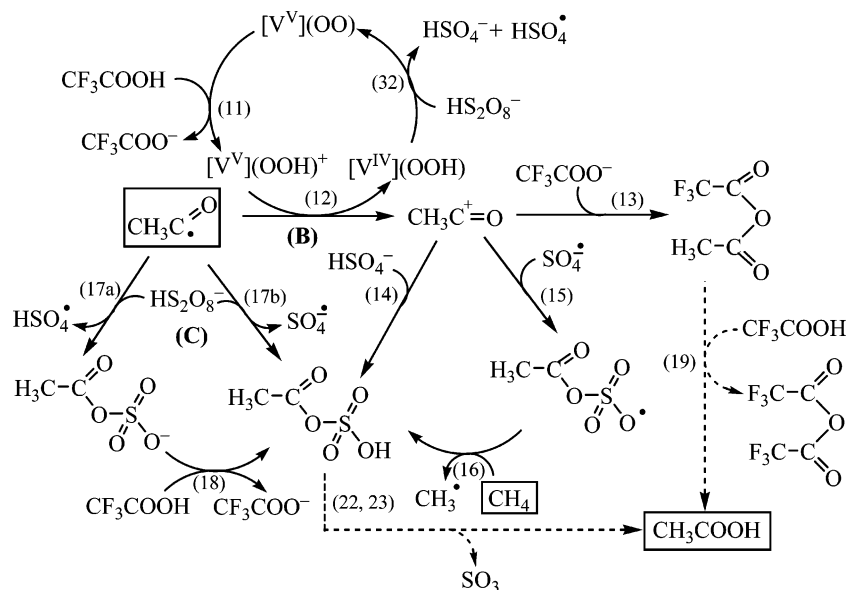
Figure 5. Equilibrium geometries of transition states and of the complexes [V(OO){N(CH₂CH₂O)₃}] and [V{OOC(O)CH₃}{N(CH₂CH₂O)₃}] involved in the main reaction mechanism of conversion of methane into acetic acid (Scheme 4).

derived from **1** ($\Delta G_s = +7.88$ kcal/mol) to give the acetate radical $\text{CH}_3\text{COO}\cdot$ (reactions 7 and 8, Scheme 4), (B) the oxidation of $\text{CH}_3\text{CO}\cdot$ by that peroxy-complex (upon protonation) to CH_3CO^+ (reactions 11 and 12, Scheme 5), and (C) the oxidation of $\text{CH}_3\text{CO}\cdot$ by peroxodisulfate (reactions 17, Scheme 5). Within the route (A) (Scheme 4), the active peroxy species ([V(OO){N(CH₂CH₂O)₃}) can be formed by reaction of the oxo-complex [VO{N(CH₂CH₂O)₃}] **1** with a peroxy-acid (reactions 7, Table 3). The plausible mechanism for such a conversion includes the initial conversion of HS_2O_8^- into peroxomonosulfuric acid H_2SO_5 , the latter (Caro's acid) being a well recognized⁶⁶ peroxidative agent. Our calculations suggest that HS_2O_8^- can in fact be decomposed by TFA ($\Delta G_s = +5.63$

kcal/mol, reactions 7a) to H_2SO_5 . Both acids, HS_2O_8^- and H_2SO_5 , should be in solution in comparable amounts, taking into account the great excess of TFA. Moreover, hydrolysis of $\text{H}_2\text{S}_2\text{O}_8$ to yield H_2SO_5 is known,⁶⁶ and thus the occurrence of this reaction, involving traces of water, cannot be ruled out.

It is noteworthy to mention that the energy of the homolytic OO bond cleavage in peroxodisulphuric acid is considerably lower than that in peroxomonosulfuric acid (22 versus 36 kcal/mol)⁶³ which can explain why the methane reaction does not proceed in the presence of H_2SO_5 instead of $\text{K}_2\text{S}_2\text{O}_8$. The peroxodisulfate has a key role in the formation of free radicals (reactions 1 and 2, Table 3) whereas the peroxomonosulfate acts, at a later stage, as an oxygen donor in the peroxidation of the catalyst (reaction 7b). In addition, the peroxidation of **1** by HS_2O_8^- (reaction 7c) cannot also be ruled out. Indeed, the

(66) *Advanced Inorganic Chemistry*, 6th ed.; Cotton, F. A., Wilkinson, G., Murillo, C. A., Bochmann, M., Eds.; John Wiley & Sons: New York, 1999; p 1356.

Scheme 5. Alternative and Less Favorable Mechanisms for the Conversion of $\text{CH}_3\text{CO}^\bullet$ to Acetic Acid [Routes (B) and (C)]^a

^a Reaction numbers correspond to those of Table 2. [V] = vanadium metal center namely $\text{V}\{\text{N}(\text{CH}_2\text{CH}_2\text{O})_3\}$.

vertical energies of the heterolytic $\text{OO}-\text{S}$ bond cleavage (70.86 kcal/mol at the $\text{CPCM-B3LYP/6-311+G}^{**}$ level) and the homolytic $\text{O}-\text{O}$ bond rupture (26.34 kcal/mol) for HS_2O_8^- are significantly lower than the energies of deprotonation and $\text{O}-\text{O}$ bond cleavage (311.61 and 49.56 kcal/mol, respectively) for H_2O_2 , and the latter is an effective peroxidizing agent. Finally, sulfate radicals were also found to be good oxygen donors.⁶⁷

The reaction of $\text{CH}_3\text{CO}^\bullet$ with $[\text{V}(\text{OO})\{\text{N}(\text{CH}_2\text{CH}_2\text{O})_3\}]$ proceeds in two steps. In the first one, the peracetate intermediate $[\text{V}\{\text{OOC}(\text{O})\text{CH}_3\}\{\text{N}(\text{CH}_2\text{CH}_2\text{O})_3\}]$ is formed via **TS3a** (Figure 5) with a low activation barrier ($\Delta H_s^\ddagger = 4.39$ kcal/mol, reaction 8a), which, on the second step, easily decomposes, via **TS3b**, into $\text{CH}_3\text{CO}^\bullet$ and the parent oxo-complex **1** that is thereby regenerated ($\Delta H_s^\ddagger = 5.98$ kcal/mol, reaction 8b). $\text{CH}_3\text{COO}^\bullet$ abstracts a hydrogen from, e.g., excess CF_3COOH or CH_4 (via **TS4** or **TS5**, reactions 9 or 10) directly affording acetic acid. The low ΔH_s^\ddagger values and high exothermicity ($\Delta H_s = -58.10$ and -15.62 kcal/mol) of reactions 8 make this route very effective in the presence of the V-catalyst. Route (A) is in fact the simplest and the most favorable one for the formation of acetic acid (see below).

Pathway (B) (Scheme 5) starts with the initial protonation of the peroxy complex $[\text{V}(\text{OO})\{\text{N}(\text{CH}_2\text{CH}_2\text{O})_3\}]$ by CF_3COOH leading to the cationic hydroperoxo- V^{V} species $[\text{V}(\text{OOH})\{\text{N}(\text{CH}_2\text{CH}_2\text{O})_3\}]^+$ (reaction 11) with an enhanced oxidizing ability. The calculated ΔH_s and ΔG_s values for this reaction are +9.13 and +8.26 kcal/mol, respectively, but the protonated complex should be formed significantly due to the great excess of the CF_3COOH solvent. The following oxidation of $\text{CH}_3\text{CO}^\bullet$ to the acyl cation $\text{CH}_3\text{C}^+=\text{O}$ by $[\text{V}(\text{OOH})\{\text{N}(\text{CH}_2\text{CH}_2\text{O})_3\}]^+$ (reaction 12) is exothermic and exoergic and leads to the reduced V^{IV} form which, upon oxidation by peroxodisulfate (reaction 32), regenerates the active oxidizing V^{V} species. The $\text{CH}_3\text{C}^+=\text{O}$ cation is involved in a number of reactions with anions present in solution (CF_3COO^- , HSO_4^- , $\text{SO}_4^{\bullet-}$) to form the mixed anhydrides $\text{CF}_3\text{C}(\text{O})\text{OC}(\text{O})\text{CH}_3$, $\text{CH}_3\text{C}(\text{O})\text{OSO}_2\text{OH}$, $\text{CH}_3\text{C}(\text{O})\text{OSO}_3^\bullet$

(reactions 13–15). The latter radical can act as an H-atom abstractor from CH_4 (reaction 16) via **TS6** (Figure 6) with a low activation barrier ($\Delta H_s^\ddagger = 2.84$ kcal/mol) and with a reaction enthalpy of -6.56 kcal/mol, thus providing an additional source of CH_3^\bullet radicals.

Within the route (C) (Scheme 5), which would not require V-catalyst, the oxidation of $\text{CH}_3\text{CO}^\bullet$ by peroxodisulfate (e.g., HS_2O_8^-) involves an attack of the former either to the sulfate peroxy-atom giving HSO_4^\bullet and the deprotonated mixed acetic/sulfuric anhydride $\text{CH}_3\text{C}(\text{O})\text{OSO}_3^-$ (reaction 17a) or to the hydrosulfate peroxy-atom forming $\text{SO}_4^{\bullet-}$ and $\text{CH}_3\text{C}(\text{O})\text{OSO}_2\text{OH}$ (reaction 17b). For both of these processes, a transition state was located (**TS7a** and **TS7b**, respectively, Figure 6), and the reactions proceed with similarly low activation barriers (ca. 5 kcal/mol) and with highly negative ΔH_s values (ca. -57 kcal/mol).

The hypothesis of *further conversions of the mixed anhydrides formed in routes (B) and (C)* has also been investigated theoretically. For reaction 19 of $\text{CF}_3\text{C}(\text{O})\text{OC}(\text{O})\text{CH}_3$ with CF_3COOH , several possible mechanisms, i.e., four concerted and one stepwise, have been considered. Two of the concerted pathways include the formation of a six-membered transition state (**TS8a** or **TS8b**, Figure 6). The former TS is derived from attack of the OH bond of CF_3COOH to the carbonyl carbon and the carbonyl oxygen of the trifluoroacetate and acetate groups, respectively, of the mixed anhydride. The latter TS is formed by attack of the carbonyl and the hydroxyl groups of CF_3COOH to the CO single bond of the trifluoroacetate moiety of the anhydride. Two other concerted pathways involve a four-membered transition state (**TS8c** or **TS8d**, Figure 6). The mechanism based on **TS8a** was found to be the least energetic one but with a relatively high activation enthalpy in solution of 26.87 kcal/mol.

Another possible mechanism for reaction 19 involves a stepwise pathway comprising the initial protonation of one of the oxygen atoms of the mixed anhydride by CF_3COOH followed by nucleophilic attack of CF_3COO^- to the carbonyl C atom of the trifluoroacetate moiety of the anhydride with

(67) Wille, U. *Chem.-Eur. J.* **2002**, *8*, 341.

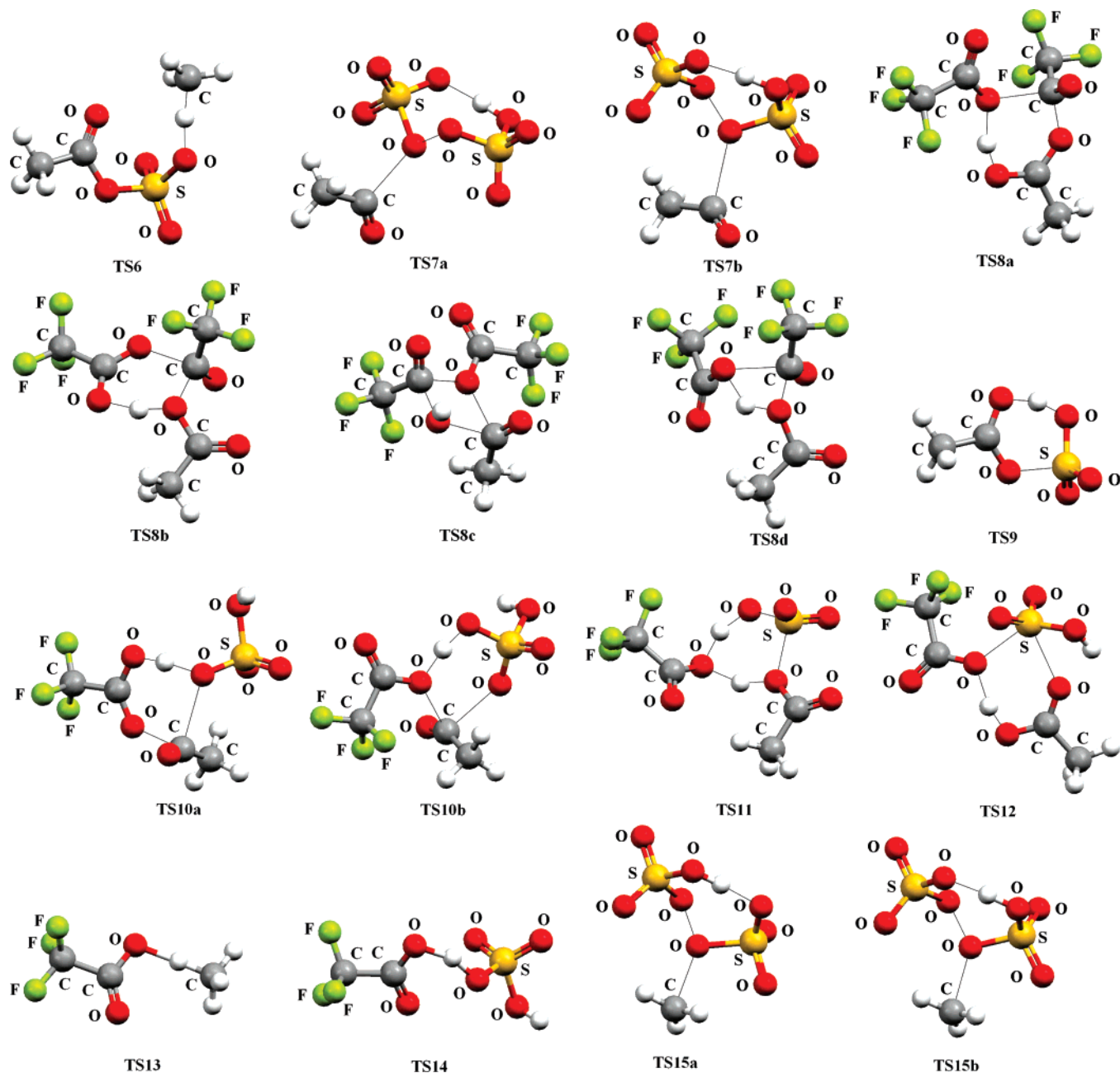


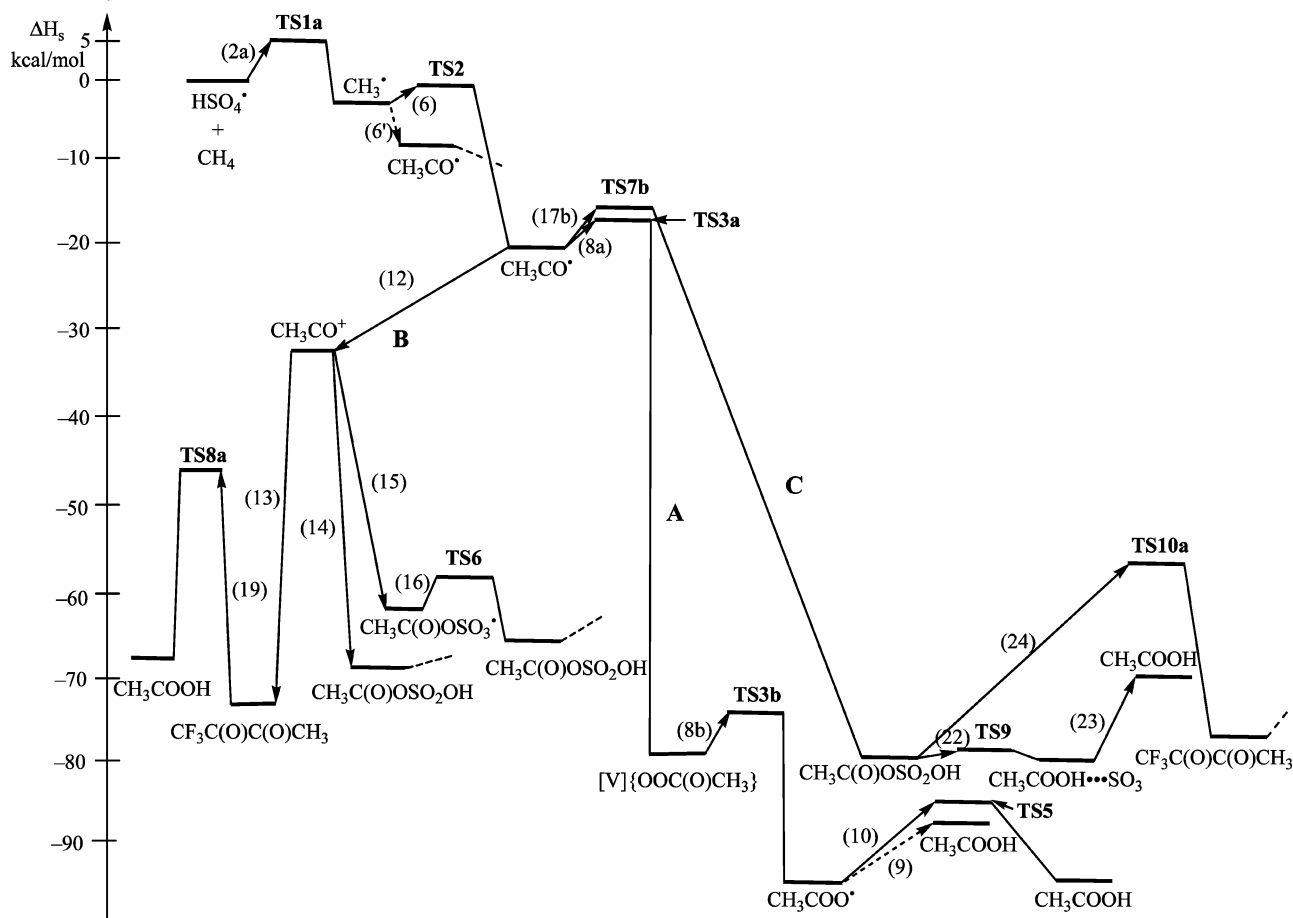
Figure 6. Equilibrium geometries of transition states involved in the alternative and less favorable mechanisms of methane carboxylation to acetic acid (reactions of Scheme 5 and the dotted ones of Scheme 4).

elimination of CH₃COOH. However, in the liquid TFA medium, this mechanism is predicted to be less favorable than the concerted route based on **TS8a**. Indeed, the protonation of the acetate carbonyl oxygen (reaction 19b) requires 41.14 kcal/mol. No minimum on PES was found for a structure protonated *via* the bridged oxygen atom. The calculations revealed that protonation of this O atom as well as of the trifluoroacetate carbonyl oxygen results in cleavage of the CO bond of the acetate moiety and elimination of CF₃COOH instead of acetic acid (reverse reaction).

Several possible ways for the conversion of the mixed anhydride CH₃C(O)OSO₃[−] or CH₃C(O)OSO₂OH into CH₃COOH have also been studied. The simple heterolytic cleavage of the SO bond to produce CH₃COO[−] and either directly SO₃ or HOSO₂⁺ followed by deprotonation to give SO₃ (reactions 20 and 21) was found to be strongly unfavored. But another

way—one-step proton migration from the sulfate O-atom of CH₃C(O)OSO₂OH to the carbonyl oxygen (reaction 22) *via* **TS9** (Figure 6)—leads, with a low activation barrier (ΔH_s^\ddagger and ΔG_s^\ddagger are 0.60 and 0.97 kcal/mol, respectively), to the adduct CH₃COOH⋯SO₃. However, the following decomposition of this adduct into individual CH₃COOH and SO₃ molecules (reaction 23) is endothermic and requires an energy of 7.16 kcal/mol.

Finally, as for reaction 19 of CF₃C(O)OC(O)CH₃, the transformations of CH₃C(O)OSO₂OH may be assisted by solvent CF₃COOH (reaction 24, Table 3), and four concerted and two stepwise mechanisms were considered. For the former, the transition states **TS10a**, **TS10b**, **TS11**, and **TS12** (Figure 6) have been located on the PES, and **TS10a** has the lowest energy corresponding to an activation barrier of 15.50 kcal/mol. The stepwise routes include the initial protonation of one of the oxygen atoms of CH₃C(O)OSO₂OH, but no minimum corre-

Scheme 6. Energy Profile for the Plausible Mechanisms Calculated at the B3LYP/6-31G* Level of Theory (Only the Most Important Species Are Indicated)

sponding to $\text{CH}_3\text{C}(\text{O})\text{OHSO}_2\text{OH}^+$, $\text{CH}_3\text{C}(\text{OH})\text{OSO}_2\text{OH}^+$, or $\text{CH}_3\text{C}(\text{O})\text{OS}(\text{O})(\text{OH})\text{OH}^+$ structure was found. Instead, protonation of the bridged O-atom results in the formation of $\text{CH}_3\text{C}(\text{OH})\text{OH}^+$ bound to SO_3 by a hydrogen bond (reaction 24d). The proton attack to the acetate carbonyl oxygen leads to weakening of the SO bond (to 1.894 Å) and formation of the adduct $\text{CH}_3\text{COOH}\cdots\text{SO}_2\text{OH}^+$ (reaction 24e). However, the energies required for both reactions are high (ca. 38 kcal/mol). The protonation of the sulfate oxygen affords H_2SO_4 and regenerates CH_3CO^+ instead of leading to acetic acid. Thus, the mixed anhydrides $\text{CH}_3\text{C}(\text{O})\text{OSO}_2\text{OH}$ and $\text{CF}_3\text{C}(\text{O})\text{OC}(\text{O})\text{CH}_3$ formed via routes (B) and (C) should be stable products under the reaction conditions, making these routes for acetic acid less favorable than (A) (Scheme 6) which proceeds via the acetate radical CH_3COO^* and does not involve mixed anhydrides. Nevertheless, the three routes can compete to some extent, a typical situation for free radical processes.

In the presence of a catalyst, the formation of acetic acid should occur predominantly via route (A), while routes (B) and (C) would lead mainly to mixed anhydrides. In the absence of a catalyst, the reaction would proceed via route (C) which would terminate with the formation of a mixed anhydride and no acetic acid would be detected in accord with the experiments.

The proposed mechanistic schemes may also qualitatively explain the effect of the oxidant amount on the yield of acetic acid (Figure 1). The increase in oxidant promotes the formation of radicals (including CH_3CO^*) and thus of acetic acid but, on the other hand, favors also route (C) that leads to an increase

of $\text{CH}_3\text{C}(\text{O})\text{OSO}_2\text{OH}$ with a concomitant decrease of CH_3COOH . The overall effect exhibits a maximum at a particular oxidant-to-catalyst ratio (ca. 120).

Side Reactions. ^{13}C -labeled methyltrifluoroacetate, $\text{CF}_3\text{COO}^{13}\text{CH}_3$, and methylsulfate, $^{13}\text{CH}_3\text{OSO}_3^-$ or $^{13}\text{CH}_3\text{OSO}_2\text{OH}$, were detected as minor products by ^{13}C NMR when starting from ^{13}C -enriched methane, in the absence of CO (reaction *b*, Scheme 2). The formation of that ester can be accounted for by the reaction of CH_3^* or HSO_4^* with CF_3COOH to give (reaction 25 or 26, Scheme 4) the CF_3COO^* radical (via **TS13** or **TS14**, Figure 6) which, upon further reaction (28) with CH_3^* , gives the ester.⁶⁸ The generation of this ester by direct H-elimination from the reaction of CH_3^* with CF_3COOH (reaction 27) would require a higher energy.

The formation of methylsulfate involves the oxidation of CH_3^* by peroxodisulfate (reactions 30a and 30b, Scheme 4) and proceeds via the transition states **TS15a** and **TS15b** (Figure 6) with a low activation barrier (7.54–7.80 kcal/mol) and with a strongly negative ΔH_s value [(-50.46) – (-56.61) kcal/mol]. Note that the oxidation of CH_3^* to CH_3^+ by peroxo-vanadium complexes (e.g., reaction 29, Table 3), a process similar to that of the oxidation of CH_3CO^* (reaction 12), is strongly unfavorable. In the presence of CO, these reactions do not compete significantly with the carbonylation of CH_3^* (reaction 6, Scheme 4) under the usual experimental conditions, and methyl trifluoroacetate or methylsulfate is detected only in very low amounts.

(68) The CH_3COO^* radical was proposed to be formed upon reaction of CH_3COO^- with $\text{SO}_4^{\cdot-}$.^{61a}

Conclusions

The direct single-pot carboxylation of methane into acetic acid by using the above vanadium complexes with N,O- or O,O-ligands as catalysts proceeds under moderate conditions and exhibits a marked selectivity toward the formation of a main single product, i.e., acetic acid, although methyltrifluoroacetate and methylsulfate appear as minor products when the reaction is performed in the absence of CO.

The results can be interpreted on the basis of radical mechanisms that have been established by theoretical calculations and radical trap experiments, in which pivotal roles played by peroxy reagents, trifluoroacetic acid, and vanadium species are evident. In particular, *peroxodisulfate* behaves as follows: (i) a source of sulfate radicals, i.e., HSO₄[•], SO₄^{•-}, and CH₃-COOSO₃[•] (the latter from coupling of SO₄^{•-} with CH₃CO⁺), which are H-atom abstractors from methane (reactions 2 and 16, Schemes 4 and 5, respectively) to yield CH₃[•] that is prone to undergo carbonylation to form CH₃CO[•] (reaction 6, Scheme 4); (ii) a peroxidative agent for vanadium to form an active peroxy-complex (reaction 7, Scheme 4); (iii) an oxidizing agent of vanadium(IV) species, e.g., leading to the regeneration (reaction 32, Scheme 5) of an active peroxy-vanadium(V) compound; (iv) an oxidizing and coupling agent for the acyl radical to give the mixed acetic/sulfuric anhydride (reaction 17, Scheme 5); (v) the source of the sulfate group in the formation of methylsulfate (minor product), upon reaction with CH₃[•] (reactions 30, Scheme 4).

Trifluoroacetic acid does not act as a mere solvent but is involved in reactions that lead to the carboxylated products. In fact, toward the formation of acetic acid, TFA (i) acts as a carbonyl source thus replacing the noxious CO gas; (ii) acts as a hydrogen source to the acetate radical to form acetic acid (reaction 9, Scheme 4); (iii) promotes the oxidizing power (toward CH₃CO[•]) of a peroxy-vanadium(V) complex (by protonation at the peroxy-ligand, reaction 11, Scheme 5); and (iv) forms a mixed trifluoroacetic/acetic anhydride (reaction 13, Scheme 5). Moreover, TFA is the source of the trifluoroacetate group in the formation of the CF₃COOCH₃ ester (minor product), upon reaction with methyl or sulfate radicals (reactions 25 and 26, Scheme 4).

Peroxy- and oxo-vanadium(V) complexes display a prominent role. A peroxy-vanadium(V) compound (derived from an oxo-precursor) can oxygenate the acyl (CH₃CO[•]) to the acetate (CH₃-COO[•]) radical via an η¹-OOC(O)CH₃ complex (reactions 8, Scheme 4) in a highly exothermic process with a low activation barrier; the formed CH₃COO[•] radical, upon H-abstraction, forms acetic acid. That peroxy-V complex, on protonation to the hydroperoxy form, can oxidize the CH₃CO[•] radical (reaction 12, Scheme 5), in a less favorable process, whereas V-species and CF₃COOH possibly play a promoting role in the decomposition of peroxodisulfate to produce SO₄^{•-} and HSO₄[•] radicals. Theoretical studies of such assisted decompositions are in progress.

The catalytic activity is significantly dependent on the ligand type, the highest one being provided by the ligands with the basic forms of triethanolamine and (*N*-hydroxyimino)dicarboxylic acids; for the former ligand, replacement, e.g., of the three or two of the ligating alkoxide arms by carboxylates or acetamide groups has an inhibitory effect. The metal oxidation state of the catalyst precursor can be either +5 or +4, and along

the reaction, the former can be attained and/or regenerated upon oxidation of the latter by the peroxy reagent.

The yield of acetic acid is dependent on a number of parameters and can reach values above 50% (or remarkable TONs up to 5.6 × 10³) for a single batch. In some cases, the catalyst is still active at the end of the reaction and the activity of the system is restored simply upon addition of additional peroxodisulfate. Accordingly, recycling of the reaction system with the addition of new portions of the peroxy-reagent and the gases (methane and carbon monoxide) for each run, but without requiring any additional catalyst or solvent, was shown to provide a method for a better utilization of these reagents. These features of the catalytic systems are of synthetic significance and deserve further exploration, although we are aware of the handicaps, from a commercial point of view, of using TFA and K₂S₂O₈ in comparison with cheaper solvents and oxidants.

The results can also be of a biological meaning since *amavadin* and its model (complexes 2 and 3, respectively) are within the most effective catalyst precursors for methane carboxylation. We thus extend to methane (the most inert alkane) and to this type of reaction the range of substrates and catalyzed reactions we have previously found for *amavadin*, i.e., oxidation of cycloalkanes,⁵⁴ of some aromatics,⁶⁹ and of a few particular biological thiols,⁷⁰ as well as carboxylation of linear and cyclic C₅ and C₆ alkanes⁷¹ and of propane.⁵² Nevertheless, the biological role of *amavadin* still remains an intriguing matter to be clarified.

Experimental Section

Caution: Particular precautions should be taken when handling CO (toxic) and the CH₄ gas that can form explosive mixtures with air. A well ventilated hood should always be used.

All synthetic work was performed under a dinitrogen atmosphere. The solvents were dried over appropriate drying agents and degassed by standard methods. Methane (Air Liquid Portugal), ¹³C-enriched methane (Aldrich), carbon monoxide (Air Products), ¹³C-enriched carbon monoxide (Aldrich) and dinitrogen gases (Air Liquid Portugal), potassium peroxodisulfate (Fluka), ammonium peroxodisulfate (Fluka), oxone (Aldrich), hydrogen peroxide solution (30% in water) (Fluka), potassium permanganate (Fluka), manganese dioxide (Merck), potassium dichromate (Aldrich), trifluoroacetic acid (TFA) (Aldrich), trichloroacetic acid (Fluka), formic acid (Aldrich), sulfuric acid (Riedel-de Haën), *n*-butyric acid (Aldrich), vanadium(V) oxide (Aldrich), vanadium(IV) oxide (Merck) and vanadyl sulfate hydrate (Merck), triethanolamine (Fluka), *N,N*-bis(2-hydroxyethyl)glycine (H₃bicine) (Aldrich), pyridine-2,6-dicarboxylic acid (H₂dipic) (Aldrich), bromoacetic acid (Merck), bromopropionic acid (Merck), nitrotriacetic acid (H₃nta) (Aldrich), *N*-2-acetamidoimino diacetic acid (H₂ada) (Aldrich), 2-hydroxyethylimino diacetic acid (H₃heida) (Aldrich), trifluoromethanesulfonic acid (Aldrich), hydroxylammonium chloride (Aldrich), zinc acetate (Aldrich), potassium methanesulfonate (Fluka), potassium methyl sulfate (Fluka), 2,6-di-*tert*-butyl-4-methylphenol (BHT) (Aldrich), 5,5-dimethyl-1-pyrroline *N*-oxide (Aldrich), bromotrichloromethane (Fluka), and diethyl ether (Lab-Scan) were obtained from commercial sources and used as received. 2,2'-(Hydroxyimino)diacetic

(69) Reis, P. M.; Silva, J. A. L.; Fraústo, da Silva, J. J. R.; Pombeiro, A. J. L. *J. Mol. Catal. A: Chem.* **2004**, *224*, 189.

(70) Guedes da Silva, M. F. C.; da Silva, J. A. L.; Fraústo da Silva, J. J. R.; Pombeiro, A. J. L.; Amatore, C.; Verpeaux, J.-N. *J. Am. Chem. Soc.* **1996**, *118*, 7568.

(71) Reis, P. M.; Silva, J. A. L.; Palavra, A. F.; Fraústo da Silva, J. J. R.; Pombeiro, A. J. L. *J. Catal.* **2005**, *235*, 333.

acid (H₃HIDA),⁷² 2,2'-(hydroxyimino)dipropionic acid (H₃HIDPA),⁷² and Caro's acid⁷³ were prepared according to published methods.

C, H, and N elemental analyses were carried out by the Microanalytical Service of the Instituto Superior Técnico. Positive-ion FAB mass spectra were obtained on a Trio 2000 instrument by bombarding 3-nitrobenzyl alcohol (NBA) matrices of the samples with 8 keV (*ca.* 1.18 × 10¹⁵ J) Xe atoms. Mass calibration for data system acquisition was achieved using CsI. Infrared spectra (4000–400 cm⁻¹) were recorded on a Jasco FT/IR-430 instrument in KBr pellets. ¹H, ¹³C-^{¹H}, and ⁵¹V NMR spectra using TMS as internal standard (for ¹³C) and VOCl₃ (for ⁵¹V) were measured on a Varian UNITY 300 spectrometer at ambient temperature.

The reaction mixture was analyzed using a Fisons Instruments GC 8000 series gas chromatograph with a DB WAX fused silica capillary column (P/N 123-7032) and the Jasco-Borwin v.1.50 software and/or using a Trio 2000 Fisons mass spectrometer with a coupled gas chromatograph Carlo Erba Instruments (Auto/HRGC/MS).

Catalyst Preparation. Complexes **1**,^{74,75} **2** (racemic mixture),⁷⁶ **3**,⁷⁶ **4**,⁷⁷ **5**,⁷⁸ **6**,⁷⁹ **7**,⁸⁰ **8**,⁸⁰ **14**,⁸¹ **15**,⁸¹ and **16**⁸² were prepared according to published methods. Compounds **11**, **12**, and **13** were obtained from a commercial source and used as received. The syntheses and characterization of complexes **9**, **10**, and **17** are described in the Supporting Information.

Catalytic Activity Studies. The reaction mixtures were prepared as follows. To 0.010–0.312 mmol of the metal complex **1**–**17** contained in a 39.0 (or 23.5 or 13.0) mL stainless steel autoclave equipped with a Teflon-coated magnetic stirring bar were added the oxidant [either K₂S₂O₈ (3.13–15.63 mmol) or (NH₄)₂S₂O₈ (6.25–18.75 mmol)] and TFA (7.3–32.0 mL). The autoclave was then closed and flushed with dinitrogen three times for displacement of the air and finally pressurized with 1.5–12.0 atm of methane and 0–30 atm of carbon monoxide. The reaction mixture was vigorously stirred using a magnetic system for 0.5–20 h and heated at 80 °C with an oil bath for the required time. The autoclave was then cooled in an ice bath, degassed, and opened. The reaction mixture was filtered off, and to a sample of 2.5 mL of the solution were added 6.5 mL of diethyl ether (which leads to further precipitation) and 90 μL of *n*-butyric acid (as internal standard). The obtained mixture was stirred, then filtered off, and analyzed by gas chromatography (GC). In some cases, the products were also identified by GC–MS and by ¹H, ¹³C, and ¹³C-^{¹H} NMR.

The experiments with various radical traps were performed at 5–8 atm of CH₄, in the presence (15 atm) or in the absence of CO, using the catalyst **1** (0–0.02 mmol), K₂S₂O₈ (4.14 mmol), TFA (7.3 mL), and any of the following radical traps in the 13 mL autoclave: BHT, CBrCl₃, or 5,5-dimethyl-1-pyrroline *N*-oxide (the radical trap/methane molar ratio was from 0.5:1 to 1:2). The other conditions were identical to those of the usual experiments (see above). In the case of CBrCl₃, the final reaction mixture was analyzed by ¹H and ¹³C NMR spectroscopies (in CDCl₃): δ 2.677 (s, CH₃Br), 4.972 (s, CH₂Br₂), 6.897 (s, CHBr₃), 3.039 (CH₃Cl), 5.192 (s, CH₂Cl₂), 2.266 (s, CH₃COOH); δ 9.681 (s, CH₃Br), 22.392 (s, CH₂Br₂).

For the first batch (stage) of the multiple recycling experiments, the amounts used were as follows: complex **1** (0.0625 mmol), K₂S₂O₈ (7.40 mmol), CH₄ (5 atm), CO (10 atm). For the following batches, identical amounts were used of CH₄ (5 atm), CO (10 atm), and, when added, K₂S₂O₈ (7.40 mmol). The reaction time for each batch was 20 h, and the other conditions were identical to those of the single experiments.

The experiments with ¹³C-enriched methane were performed for P¹³CH₄ = 1.5–2 atm, in the absence or in the presence of CO, i.e., P_{CO} = 0 or 20 atm, respectively, using catalyst **1** (0.50 mmol) and K₂S₂O₈ (10.0 mmol), in CF₃COOH (5.0 mL), at 80 °C (20 h reaction time). ¹³C NMR of the final reaction solution: δ 20.79 (q, J_{CH} = 130.3 Hz; ¹³CH₃COOH), 56.02 (q, J_{CH} = 150.9 Hz; CF₃COO¹³CH₃) (only traces for P_{CO} = 20 atm), 57.12 (q, J_{CH} = 149.5 Hz; ¹³CH₃OSO₂O⁻) (only traces for P_{CO} = 20 atm), 40.06 (q, J_{CH} = 136.4 Hz; ¹³CH₃SO₂O⁻) (only traces for P_{CO} = 0 atm). For P_{CO} = 20 atm, the additional weak resonance at 27.80 was not identified, being ascribed to a product of a side reaction occurring for low methane pressures. The formation of CH₃OSO₂O⁻ and CH₃SO₂O⁻ is corroborated by the identity of the δ and J_{CH} values in the ¹³C NMR spectrum of the reaction mixture with those of an authentic sample of KCH₃OSO₂O and KCH₃SO₂O in TFA solution.

The experiments with ¹³C-enriched carbon monoxide were performed for P¹³CO = 2 atm and P_{CH₄} = 5 atm, using catalyst **1** (0.020 mmol) and K₂S₂O₈ (4.0 mmol), in CF₃COOH (5.0 mL), contained in a 13 mL stainless steel autoclave equipped with a Teflon-coated magnetic stirring bar, at 80 °C (20 h reaction time). ¹³C NMR of the final reaction solution: 20.56 (weak, q, J_{CH} = 130.3 Hz; CH₃¹³COOH), 180.96 (strong, s, CH₃¹³COOH); weak resonances at 14.31 and 67.29 are ascribed to products of side reactions occurring for low CO pressure.

Quantitative Determination of CO₂. A typical carboxylation reaction of methane (10 atm, 2.13 mmol) was performed for 20 h with catalyst **1** (0.10 mmol), K₂S₂O₈ (4.2 mmol), and TFA (7.3 mL) in a 13 mL autoclave, in the presence of CO (15 atm, 3.19 mmol) or in its absence. After the resulting reaction mixture was cooled, the gas phase was displaced by dinitrogen and slowly bubbled through a clear saturated aqueous solution of Ba(OH)₂, leading to the formation of a white precipitate of BaCO₃. This was filtered off, dried in vacuo, and weighted: 0.1305 g (0.66 mmol) or 0.0395 g (0.20 mmol), in the presence or in the absence of CO, respectively.

Computational Details

The full geometry optimization of all structures and transition states has been carried out at the DFT level of theory using Becke's three-parameter hybrid exchange functional⁸³ in combination with the gradient-corrected correlation functional of Lee, Yang, and Parr⁸⁴ (B3LYP) with the help of the Gaussian 98⁸⁵ program package. The restricted approximations for the structures with closed electron shells and the unrestricted methods for the structures with open electron shells have been employed. For pure organic reactions, the 6-31G*⁸⁶ and 6-311+G**⁸⁷ basis sets were applied. For reactions involving vanadium species, a relativistic Stuttgart pseudopotential described 10 core electrons and the appropriate contracted basis set (8s7p6d1f)/[6s5p3d1f]⁸⁸ for the vanadium atom and the 6-31G* basis set for other atoms were used. Further, this level is also denoted as B3LYP/6-31G* despite the usage of the other basis set on the V atom. Symmetry operations were not applied for all structures.

- (72) Koch, E.; Kneifel, H.; Bayer, E. *Z. Naturforsch., B: Chem. Sci.* **1986**, *41*, 359.
 (73) *The Merck Index*; Budavari, S., O'Neil, M. J., Smith, A., Heckelman, P. E., Eds.; Merck & Co., Inc.: Rahway, NJ, 1989.
 (74) Root, C. A.; Hoeschele, J. D.; Corman, C. R.; Kampf, J. W.; Pecoraro, V. L. *Inorg. Chem.* **1993**, *32*, 3855.
 (75) Crans, D. C.; Chen, H.; Anderson, O. P.; Miller, M. M. *J. Am. Chem. Soc.* **1993**, *115*, 6769.
 (76) Berry, R. E.; Armstrong, E. M.; Beddoes, R. L.; Collison, D.; Ertok, S. N.; Helliwell, M.; Garner, C. D. *Angew. Chem., Int. Ed.* **1999**, *38*, 795.
 (77) Da Silva, J. A. L. Ph.D. thesis, Instituto Superior Técnico (Portugal), 1992.
 (78) Chen, C. T., et al. *Org. Lett.* **2001**, *3*, 3729.
 (79) Nishizawa, M.; Saito, K. *Inorg. Chem.* **1980**, *19*, 2284.
 (80) Hamstra, B. J.; Houseman, A. L. P.; Colpas, G. J.; Kampf, J. W.; LoBrutto, R.; Frisch, W. D.; Pecoraro, V. L. *Inorg. Chem.* **1997**, *36*, 4866.
 (81) Smith, P. D.; Harben, S. M.; Beddoes, R. L.; Helliwell, M.; Collison, D.; Garner, C. D. *J. Chem. Soc., Dalton Trans.* **1997**, 685.
 (82) Yadav, H. S.; Armstrong, E. M.; Beddoes, R. L.; Collison, D.; Garner, C. D. *J. Chem. Soc., Chem. Commun.* **1994**, 605.

- (83) Becke, A. D. *J. Chem. Phys.* **1993**, *98*, 5648.
 (84) Lee, C.; Yang, W.; Parr, R. G. *Phys. Rev.* **1988**, *B37*, 785.
 (85) Frisch, M. J., et al. *Gaussian 98*, revision A.9; Gaussian, Inc.: Pittsburgh, PA, 1998.
 (86) (a) Ditchfield, R.; Hehre, W.; Pople, J. A. *J. Chem. Phys.* **1971**, *54*, 724. (b) Hehre, W. J.; Ditchfield, R.; Pople, J. A. *J. Chem. Phys.* **1972**, *56*, 2257. (c) Hariharan, P. C.; Pople, J. A. *Theor. Chim. Acta* **1973**, *28*, 213.
 (87) (a) McLean, A. D.; Chandler, G. S. *J. Chem. Phys.* **1980**, *72*, 5639. (b) Krishnan, R.; Binkley, J. S.; Seeger, R.; Pople, J. A. *J. Chem. Phys.* **1980**, *72*, 650.
 (88) Dolg, M.; Wedig, U.; Stoll, H.; Preuss, H. *J. Chem. Phys.* **1987**, *86*, 866.

The Hessian matrix was calculated analytically for all optimized structures in order to prove the location of correct minima (no “imaginary” frequencies) or saddle points (only one negative eigenvalue) and to estimate the thermodynamic parameters; the latter were calculated at 80 °C and pressure of 10 atm. The nature of all transition states was investigated by the analysis of vectors associated with the “imaginary” frequency. The entropic terms and therefore the Gibbs free energies of activation and reaction calculated using the standard expressions for an ideal gas are overestimated or underestimated for reactions occurring in solution and proceeding with a change of number of molecules. Hence, the ΔG_s values are indicated only for the processes keeping the total number of the molecules during reaction. For the same reason, the ΔG_s^\ddagger value is indicated only for the unimolecular reaction of decomposition of CH₃C(O)OSO₂OH.

Solvent effects were taken into account at the single-point calculations on the basis of the gas-phase geometries at the CPCM-B3LYP/6-31+G**/gas-B3LYP/6-31G* and CPCM-B3LYP/6-311+G**/gas-B3LYP/6-311+G** levels of theory using the polarizable continuum model⁸⁹ in the CPCM version.⁹⁰ The trifluoroacetic acid taken as a solvent was approximated by the values of the dielectric constant and solvent radius of 8.55 and 2.18 Å, respectively. The enthalpies and Gibbs free energies in the solution (H_s and G_s) were estimated by addition of the solvation energy ΔG_{solv} to gas-phase enthalpies and Gibbs free energies (H_g and G_g).

(89) Tomasi, J.; Persico, M. *Chem. Rev.* **1997**, *94*, 2027.

(90) Barone, V.; Cossi, M. *J. Phys. Chem.* **1998**, *102*, 1995.

For some structures, several possible conformations or coordination modes have been calculated, and only the most stable ones are discussed.

Acknowledgment. This work has been partially supported by the Fundação para a Ciência e a Tecnologia (FCT) and its POCI 2010 program (FEDER funded), Portugal. M.V.K., P.M.R., and M.L.K. are grateful to the FCT (Grants BD/12811/03 and BPD/16369/98//BPD/5558/2001) and the POCTI program for fellowships (POCTI/QUI/43415/2001 and POCTI/QUI/14/2001). Prof. A. F. Palavra (IST) and Prof. Y. Fujiwara (Kyushu University) are gratefully acknowledged for the generous help and advice in setting-up the original reactor system and the latter also for stimulating discussions at the earlier stage of the work. We also thank Jiangsu Sopo Corporation Ltd. for a cooperation agreement.

Supporting Information Available: Complete refs 78 and 85. The full data on methane carboxylation, Cartesian atomic coordinates of the equilibrium structures, their total energies, enthalpies and Gibbs free energies; multiple recycling scheme, time effect for catalyst **1**, the syntheses and characterization of complexes **9**, **10**, and **17**. This material is available free of charge via the Internet at <http://pubs.acs.org>.

JA072531U